Article

Cell Reports

A Forward Genetic Screen Targeting the Endothelium Reveals a Regulatory Role for the Lipid Kinase Pi4ka in Myelo- and Erythropoiesis

Graphical Abstract

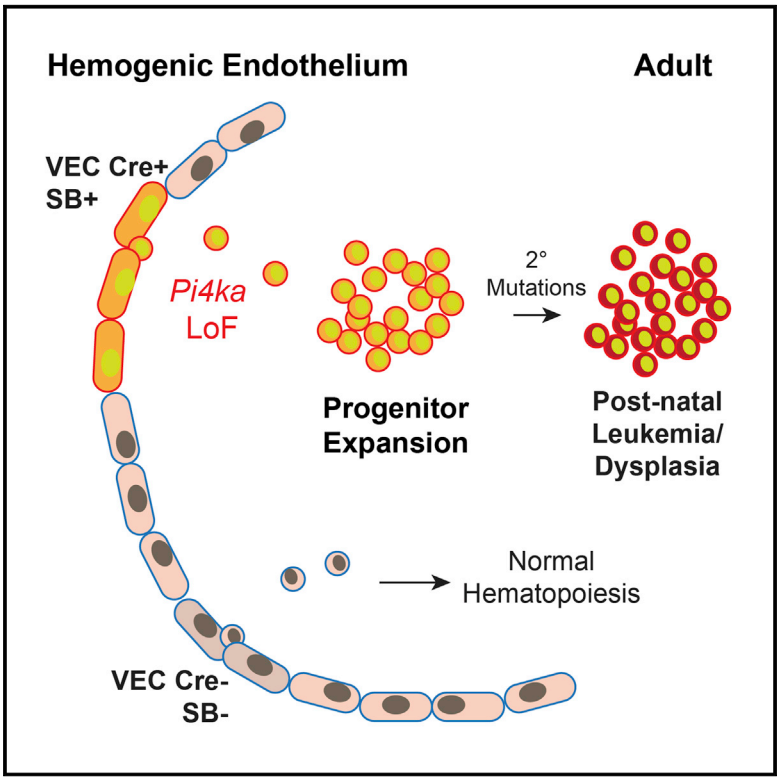

Authors

Safiyyah Ziyad, Jesse D. Riordan, Ann M. Cavanaugh, ..., Jau-Nian Chen, Adam J. Dupuy, M. Luisa Iruela-Arispe

Correspondence

arispe@mcdb.ucla.edu

In Brief

Using transposon mutagenesis that targets the endothelium, Ziyad et al. identify Pi4ka as an important regulator of hematopoiesis. Loss of Pi4ka inhibits myeloid and erythroid cell differentiation. Previously considered a pseudogene in humans, *PI4KAP2* is shown to be protein-coding and a negative regulator of PI4KA signaling.

Highlights

- Initiation of mutagenesis in the hemogenic endothelium yields hematopoietic malignancy
- Pi4ka is expressed in hematopoietic stem progenitor cells
- Pi4ka has a regulatory role in myelo- and erythropoiesis
- PI4KAP2 is a protein-coding negative regulator of Pi4ka signaling

Data and Software Availability

GSE108355

Ziyad et al., 2018, Cell Reports *22*, 1211–1224
January 30, 2018
https://doi.org/10.1016/j.celrep.2018.01.017

Cell Reports
Article

A Forward Genetic Screen Targeting the Endothelium Reveals a Regulatory Role for the Lipid Kinase Pi4ka in Myelo- and Erythropoiesis

Safiyyah Ziyad,[1] Jesse D. Riordan,[2] Ann M. Cavanaugh,[1] Trent Su,[3] Gloria E. Hernandez,[5] Georg Hilfenhaus,[1] Marco Morselli,[3,4] Kristine Huynh,[1] Kevin Wang,[1] Jau-Nian Chen,[1] Adam J. Dupuy,[2] and M. Luisa Iruela-Arispe[1,5,6,7,*]
[1]Department of Molecular, Cell, and Developmental Biology, University of California, Los Angeles, Los Angeles, CA 90095, USA
[2]Department of Anatomy and Cell Biology, University of Iowa, Iowa City, IA 52242, USA
[3]Institute for Quantitative and Computational Biology and Department of Biological Chemistry, University of California, Los Angeles, Los Angeles, CA 90095, USA
[4]Institute of Genomics and Proteomics, University of California, Los Angeles, Los Angeles, CA 90095, USA
[5]Molecular Biology Institute, University of California, Los Angeles, Los Angeles, CA 90095, USA
[6]Jonsson Comprehensive Cancer Center, University of California, Los Angeles, Los Angeles, CA 90095, USA
[7]Lead Contact
*Correspondence: arispe@mcdb.ucla.edu
https://doi.org/10.1016/j.celrep.2018.01.017

SUMMARY

Given its role as the source of definitive hematopoietic cells, we sought to determine whether mutations initiated in the hemogenic endothelium would yield hematopoietic abnormalities or malignancies. Here, we find that endothelium-specific transposon mutagenesis in mice promotes hematopoietic pathologies that are both myeloid and lymphoid in nature. Frequently mutated genes included previously recognized cancer drivers and additional candidates, such as *Pi4ka,* a lipid kinase whose mutation was found to promote myeloid and erythroid dysfunction. Subsequent validation experiments showed that targeted inactivation of the Pi4ka catalytic domain or reduction in mRNA expression inhibited myeloid and erythroid cell differentiation *in vitro* and promoted anemia *in vivo* through a mechanism involving deregulation of AKT, MAPK, SRC, and JAK-STAT signaling. Finally, we provide evidence linking *PI4KAP2,* previously considered a pseudogene, to human myeloid and erythroid leukemia.

INTRODUCTION

The hematopoietic lineage emerges during a narrow developmental window from a specialized subset of endothelial cells: the hemogenic endothelium (HemEnd) (Dzierzak and de Pater, 2016). Hematopoietic stem progenitor cells (HSPCs) enter the circulation from HemEnd sites to first seed and expand the fetal liver and later occupy the bone marrow.

The specification of the HemEnd requires *Etv2* and *Runx1,* while HSPCs budding from the HemEnd involves *Gata2*, *Jagged1-Notch*, and *Hedgehog* (Clements and Traver, 2013; Eliades et al., 2016). In recent years, the field has come to appreciate the diversity, repopulation capacity, and plasticity of single hematopoietic stem cells (HSCs) at the HemEnd stage, meaning before their seeding in hematopoietic organs (Guibentif et al., 2017). For example, VE-Cadherin-expressing HemEnd gives rise to myeloid-erythroid biased HSPCs (Chen et al., 2011), while TGF-β and BMP signaling differentially activate myeloid versus lymphoid-biased HSCs (Challen et al., 2010; Crisan et al., 2015). It is well known that lineage-specific transcription factors that drive specification of blood cells (CEBPa, Ikaros, MLL, SCL, Etv6, etc.) can lead to leukemia when deregulated (Orkin and Zon, 2008). Similarly, genes involved in the regulatory process that control budding of HSCs from the HemEnd might also promote neoplastic transformation when disrupted.

Seeking to expand our current understanding of the genes that regulate hematopoiesis (and their potential transformation) starting as early as HSPC budding, we performed a forward genetic screen using *Sleeping Beauty* (SB) transposon mutagenesis to target the HemEnd. On insertion into the genome, transposons disrupt splicing and expression of targeted genes, causing both gain- and loss-of-function events and facilitating the discovery of oncogenes and tumor suppressors in a variety of solid and blood cancers (Moriarity and Largaespada, 2015). HemEnd-initiated SB transposon mutagenesis yielded myeloid, erythroid, and lymphoid malignancies with mutations in both well-known regulators of those lineages and candidate genes uncovered in this study. Among these candidates, we identified a previously unknown role for phosphatidyl inositol lipid kinase (Pi4ka) in erythroid and myelopoiesis. Recurrent *Pi4ka* mutations were previously identified in histiocytic sarcomas driven by SB mutagenesis in cells expressing a myeloid-specific Lyz-Cre transgene, but no causative mechanisms were reported (Been et al., 2014). A lipid kinase that phosphorylates phosphatidyl-inositols at the D4 position, the Pi4ka protein may be important in a broad array of biological processes, including signaling complexes, ion channel activity, lipid transfer, vesicle transport, and actin binding (Balla et al., 2009; Minogue and Waugh, 2012). Here, we validated Pi4ka's biological significance in

hematopoiesis and demonstrated its link to Akt and Erk signaling, the former classically known to regulate hematopoietic differentiation. Furthermore, we identified the human PI4KA "pseudogene," PI4KAP2, as a dominant-negative inhibitor of the PI4KA signaling pathway.

RESULTS

HemEnd Mutagenesis Promotes Hematopoietic Malignancies

We targeted mutagenesis to the endothelium using a conditional SB transposon strategy (Dupuy et al., 2009) (Figures 1A and 1B). VE-Cadherin-Cre (VEC-Cre) recombinase (Alva et al., 2006) was used to drive expression of the transposase enzyme specifically in endothelial cells, where it could cut and paste transposons randomly into TA dinucleotides distributed throughout the genome (Riordan et al., 2014). VEC-Cre is first expressed in the HemEnd by embryonic day (E) 9.5 in a salt-and-pepper manner with progressive penetration and homogeneous expression by E12.5 (Alva et al., 2006). Due to this mosaic expression pattern in the HemEnd (transient phase lasting from E10.5–E12.5) by E10.5, some cells were targeted by mutagenesis while others were not, creating a competitive mixture of mutated and non-mutated populations.

Whereas a previous SB screen targeting HSCs using Vav-Cre (Berquam-Vrieze et al., 2011) yielded only lymphoid leukemia, the VEC-Cre screen generated both myeloid and lymphoid malignancies. A total of 76 Cre^+ and 15 Cre^- (non-mutagenized) mice were evaluated, with 59 Cre^+ and 0 Cre^- mice presenting with pathology. From this cohort, 55.3% (n = 42) developed hematopoietic abnormalities alone, 9.2% (n = 7) developed vascular anomalies, and 13.2% (n = 10) developed a combination of both (Figure 1Ci). Mice with hematopoietic abnormalities were further categorized into those with an enlarged spleen (65.4%, n = 34), an enlarged thymus (13.5%, n = 7), or both (21.2%, n = 11) (Figure 1Cii). Overall, mutagenized mice had a mean survival of 179 days (Figure 1D). An enlarged thymus was associated with faster disease kinetics compared with splenomegaly (mean survival of 139 days versus 161 days, respectively) (Figure 1E). Representative images of pathology are shown in Figure 1F. Affected mice had ~4- to 7-fold increased white blood cell counts compared with Cre^- littermates (Figure 1G) and frequently exhibited anemia (reduced red blood cell [RBC] count and hemoglobin [Hg] concentration) and increased RBC size (mean corpuscular volume [MCV]) (Figure 1H). Although affected mice commonly had abnormal platelet counts compared with Cre^- animals, no differences were observed based on the primary affected site (Figure 1I). Overall, the findings indicate that targeted mutagenesis initiated in the HemEnd results in hematopoietic malignancies.

Spleen and Thymus Malignancies Have Distinct Mutation Signatures

The SB mutagenesis system enables precise genomic coordinates of transposon-induced mutations to be determined using linker-mediated PCR and Illumina next-generation sequencing (Brett et al., 2011). Subsequent statistical analyses identified recurrently mutated regions containing clonally expanded transposon insertions at a higher rate than would be predicted in the absence of selective pressure. Because these analyses assumed a random transposition pattern, we first confirmed the unbiased distribution of insertions across all chromosomes in affected spleen and thymus DNA samples (Figures S1A–S1C). Indeed, our data were consistent with the well-established unbiased nature of SB screens in general (Bard-Chapeau et al., 2014; Dupuy et al., 2009; Keng et al., 2009; Riordan et al., 2014). We next used gene-centric common insertion site (gCIS) analysis to identify clusters of clonally expanded insertions enriched near protein coding regions. Interestingly, the number of gCISs associated with the thymus phenotype was double that of the spleen phenotype, despite the same average number of total insertions per sample (Figures S1D and S1E), supporting the concept that the cell of origin influences gCIS mutations, which in turn influences malignancy (Berquam-Vrieze et al., 2011).

Our screen activated transposon-mediated mutagenesis in the HemEnd and thus early definitive HSCs. A comparison of the gCIS list with recurrently mutated genes identified in blood cancers arising from global (non-tissue specific) and Vav-Cre-(HSPC)-driven mouse mutagenesis screens revealed substantial overlap, highlighting the ability of this approach to identify genes relevant to lymphoid malignancies (Figure 2A; Tables S1 and S2; Figure S1F). Of note, previous HSPC-targeting screens were not also able to generate myeloid malignancies without mutant JAK sensitization.

The most commonly mutated genes for the enlarged thymus phenotype were *Rasgrp1*, *Akt1*, and *Akt2*, with insertions often occurring concurrently in the same lesion (Figures 2B and 2C). Additional frequently mutated genes included *Notch1* and *Myc* (Figure 2B). Many of the genes identified in this cohort have been previously associated with T cell malignancy (Manabe et al., 2006; Oki et al., 2011; Rasmussen et al., 2009).

Frequently mutated genes in enlarged spleens were *Eras*, *Erg,* and *Ets1*, which occurred in ~40% of samples (Figures 2D and 2E). Other recurrently mutated genes included *Fli1*, *Epo*, and *Runx2* (Figure 2E). Interestingly, several genes were commonly found together in a single spleen, suggestive of a cooperative function in transformation, and included: *Eras, Erg,* and *Epo*; *Erg* and *Ets1*; and *Fli1* and *Runx2* (Figure 2F). These genes have been implicated in pathological myelo-erythropoiesis and hematopoiesis in general, providing strong validation to the screen (Athanasiou et al., 2000; Huang et al., 2009; Zochodne et al., 2000). Interestingly, malignancies resulting from HemEnd-initiated mutagenesis frequently contained mutations in genes like *Pi4ka*, *Erg,* and *Fli1*, which are more highly expressed in HSCs compared with other hematopoietic progenitor cells (Figures 2G–2I) (Chacon et al., 2014). Most splenomegaly associated mutations were also correlated with abnormal blast-like cells in the blood and reduction in polymorphonuclear cells in the bone marrow (Figures S2A and S2B).

Pi4ka Insertion Is Associated with Progenitor Accumulation and Reduced RBCs

We next focused on *Pi4ka*, which, unlike most of the genes identified by the screen, had not been previously associated with hematopoietic abnormalities or hematopoiesis in general. The three *Pi4ka* transposon insertions (each from a distinct individual)

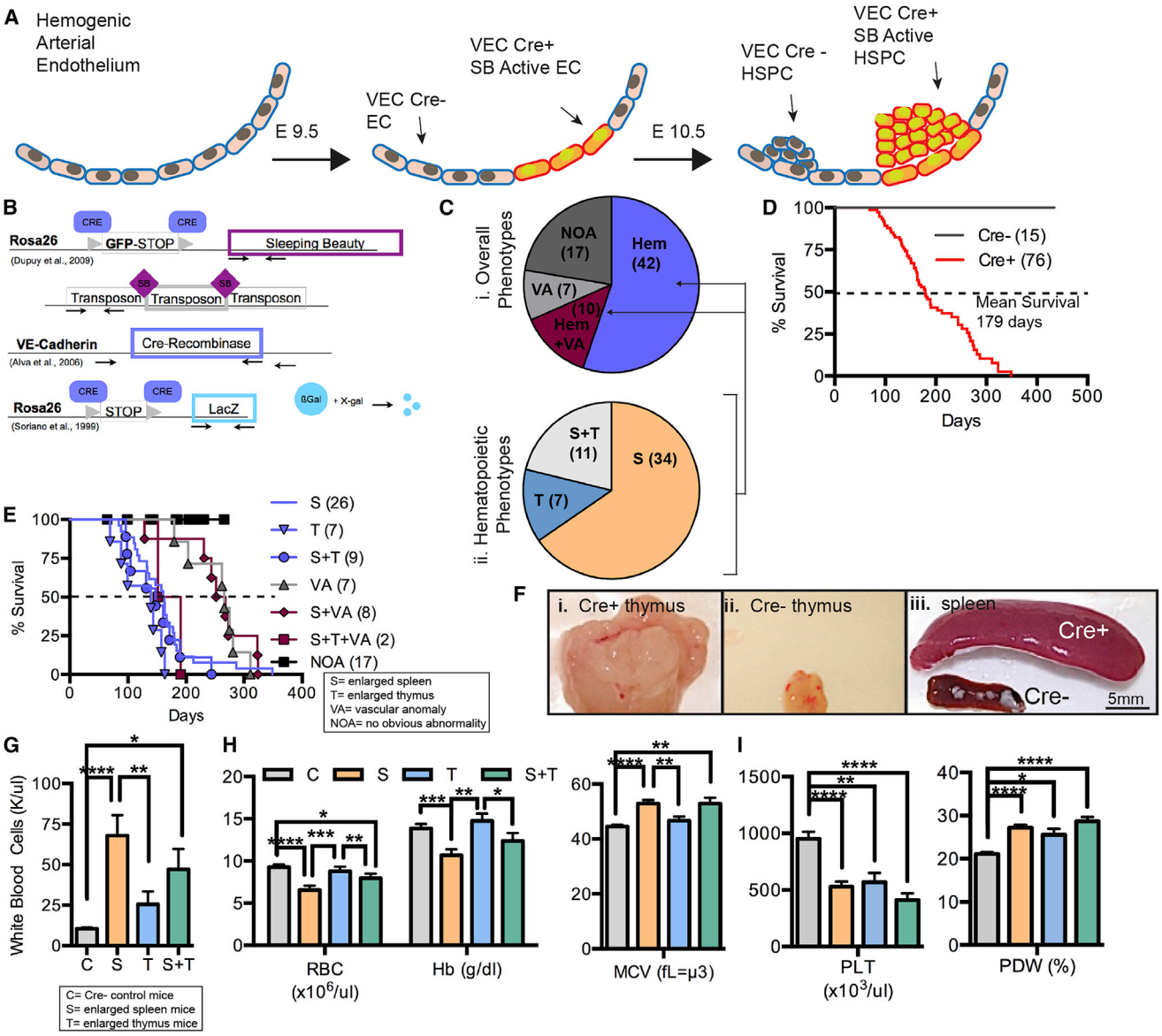

Figure 1. Initiating Mutagenesis in the Hemogenic Endothelium Generates Hematopoietic Malignancies

(A and B) Onset of VE-Cadherin-Cre (VEC-Cre) expression, and therefore SB Transposase, at E9.5 in the progeny of (B) SB T2/Onc2; VEC-Cre/Rosa26-LacZ mice.

(C) Frequencies of abnormalities in these mice (i). Relative occurrence of enlarged spleens and thymus (ii).

(D) Overall survival of Cre+ and Cre$^-$ mice (number of mice in parentheses).

(E) Kaplan-Meier curve breakdown of animals with indicated maladies.

(F) Cre$^+$ enlarged thymus (i), Cre$^-$ normal thymus (ii), Cre$^+$ enlarged spleen and Cre$^-$ normal spleen (iii). Scale bar, 5 mm.

(G) White blood cell counts for Cre$^+$ animals with enlarged spleens (S; n = 24), enlarged thymus (T; n = 5), or a combination of both (S+T; n = 10), Cre$^-$ littermates (n = 10).

(H) Red blood cell (RBC) concentration, hemoglobin (Hb) concentration, and mean cell volume (MCV) for Cre$^+$ animals with an enlarged spleen (S; n = 24), thymus (T; n = 5), or both (S+T; n = 10) compared with Cre$^-$ controls (Cs; n = 10).

(I) Platelet concentrations (PLT) and platelet distribution width (PDW%) in S, T, S+T, and C animals.

(G–I) Data are represented as mean ± SEM, Student's t test (*$p \leq 0.05$; **$p \leq 0.01$; ***$p \leq 0.001$; ****$p \leq 0.0001$) S, enlarged spleen; T, enlarged thymus; C, Cre negative; VT, vascular tumors; NOA, no obvious abnormalities; Hem, hematopoietic malignancy; HSPC, hematopoietic stem progenitor cell; Hb, hemoglobin; MCV, mean corpuscular volume; PLT, platelet count; PDW%, size distribution of platelet width.

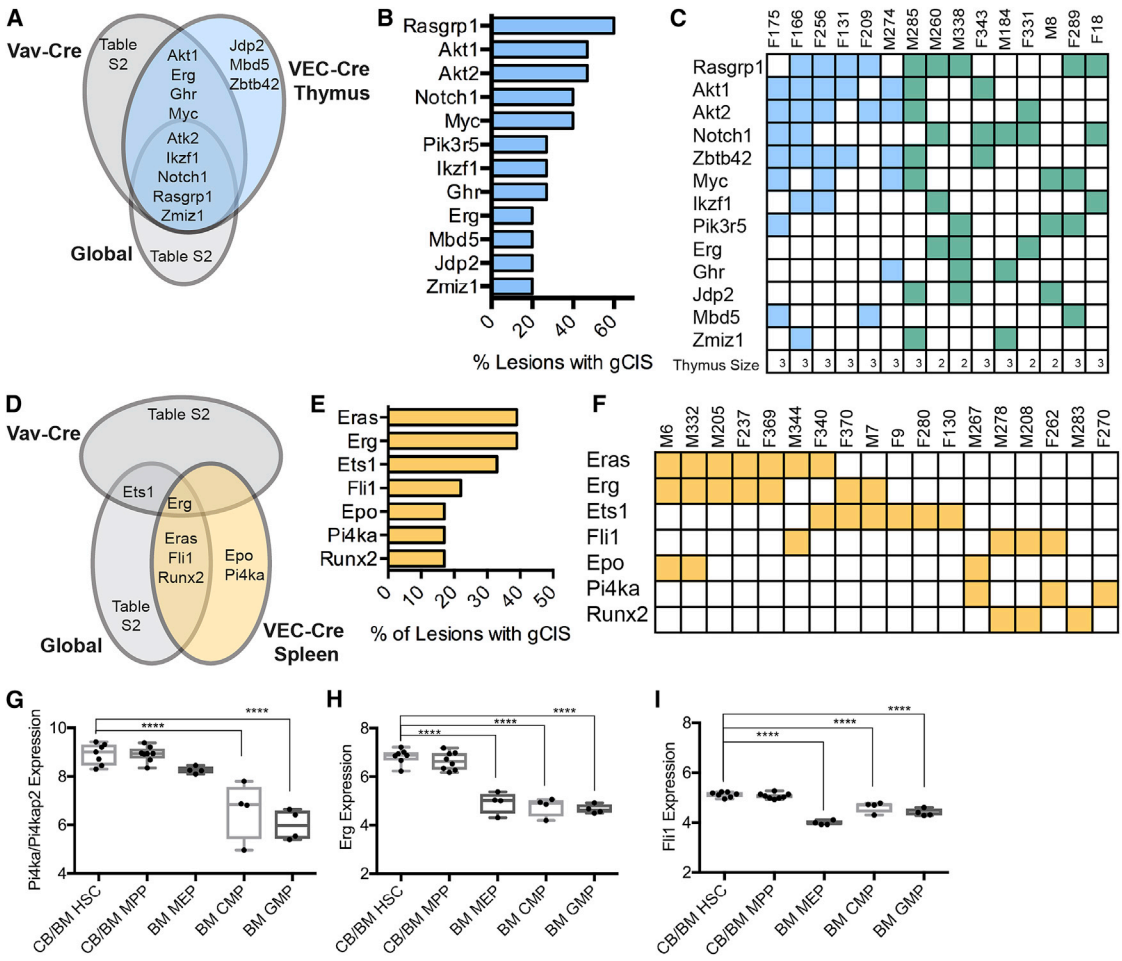

Figure 2. Thymus and Spleen Malignancies Have Distinct Gene Insertion Signatures

(A) gCIS associated with thymic abnormalities in this screen when compared with others.

(B) Most commonly mutated genes in enlarged thymus.

(C) Distribution of mutated genes (rows) in each mouse (column). F, female; M, male. The number relates to the ID of the individual mouse. Enlarged thymus phenotype is shown in blue, enlarged spleen and thymus are depicted in green. Size of the thymus is shown at the bottom as a reference (3 > 500 mg, 500 > 2 > 100 mg, 1 < 100 mg).

(D) gCIS associated with splenic abnormalities in this screen compared with other screens.

(E) Most common gCISs in enlarged spleens.

(F) Several genes (rows) were often found together in the same lesion (column).

(G–I) mRNA expression as measured by microarray of myeloid-associated gCIS *Pi4ka* (G), *Erg* (H), and *Fli1* (I) in different compartments from human bone marrow (BloodChIP); one-way ANOVA (*$p \leq 0.05$; **$p \leq 0.01$; ***$p \leq 0.001$; ****$p \leq 0.0001$). n = 4–8 per group.

See also Figures S1 and S2.

were distributed throughout the gene in both transcriptional orientations (Figure 3A), a pattern suggestive of inactivating mutations (Copeland and Jenkins, 2010). Consistent with this hypothesis, the mutations were associated with decreased *Pi4ka* mRNA (Figures 3B and 3C), and immunohistochemical analyses indicated a significant decrease of Pi4ka protein compared with controls (Figure 3D). Histological evaluation of affected spleens also revealed expanded red pulp zones compared with Cre^- spleens (Figure 3D). May-Grunwald stain of white blood cells from mice with *Pi4ka* insertions showed a prevalence of myeloid lineage, nucleated erythroid lineage, and blast-like immature cells (Figure 3D, bottom). Strikingly, when the *Pi4ka* insertion occurred in the absence of additional gCIS mutations (F270), the predominant cell type was blast-like and immature, which was also associated with anemia (Figures 3D [bottom] and 3E). On the other hand, when the *Pi4ka* mutation occurred in the same lesion as either the *Epo* or *Fli1* mutation, lesions appeared myelodysplastic and were characterized by an abundance of nucleated erythroid lineage cells (Figure 3D, bottom).

Pi4ka Insertions Are Associated with Impaired Myelo- and Erythropoiesis

To assess the cellular composition and clonality of spleens with *Pi4ka* mutations, we first performed transcriptome

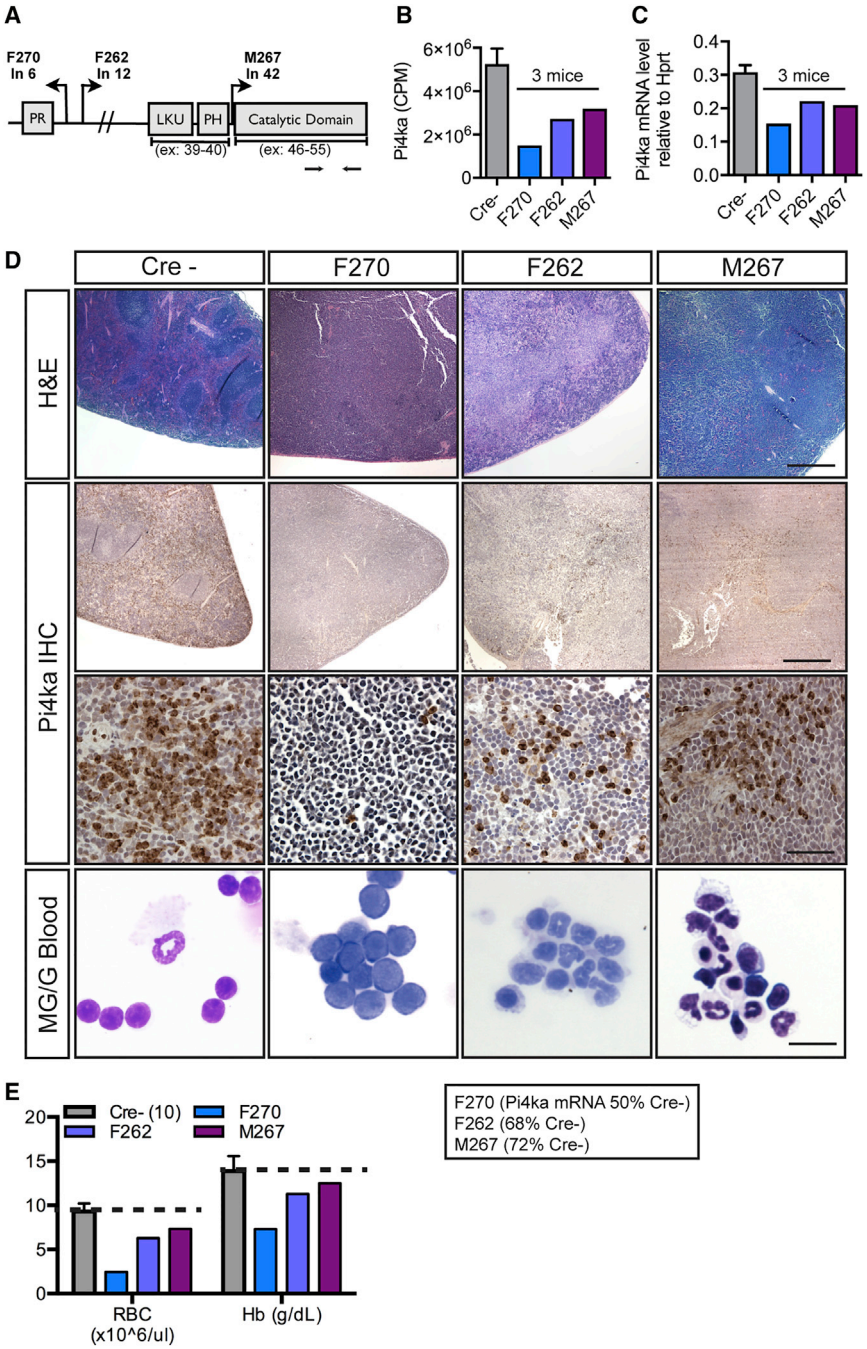

Figure 3. Transposon Insertions in the *Pi4ka* Gene Are Associated with Blast-like Phenotype and Decreased Red Blood Cells

(A) Transposon insertions throughout the *Pi4ka* gene.

(B) *Pi4ka* RNA sequencing counts per million for affected and C spleens.

(C) *Pi4ka* expression by qPCR of the individual spleens from affected mice compared to Cre$^-$ spleens (n = 6).

(D) H&E of Cre$^-$ spleens and those with *Pi4ka* insertions (scale bar, 600 μm). Pi4ka immunohistochemistry (IHC) in spleens of C and affected mice (top: scale bar, 600 μm; middle: scale bar, 60 μm). Bottom: Cytospins of RBC-lysed blood from C and affected animals (scale bar, 15 μm)

(E) CBC analysis in C and *Pi4ka*-affected animals. For Cs (Cre$^-$), data are represented as mean ± SEM of n = 10 animals.

analysis of both mutant and control spleens (Figure 4A). Based on the expression of cell-type-specific markers (Zhu and Emerson, 2002), *Pi4ka* mutant spleens had less lymphocytic, more HSCs, and more common myeloid progenitor (CMP) features when compared with controls. Animal F270 had the least mature monocyte-macrophage character, both F270 and F262 had increased granulocyte-monocyte progenitor (GMP) features, and both F270 and M267 had decreased mature erythroid hemoglobin transcripts. These results led us to hypothesize that Pi4ka might have a role in erythroid and myeloid maturation. Consistently, downregulated genes were enriched for Gene Ontology categories related to mature blood cells markers (Figure 4B), and upregulated genes were enriched for categories related to cell proliferation (Figure 4C). Expression of the genes defined in Figure 4A revealed strong similarity between two independent regions of each affected and control spleen (Pearson correlation; diagonal) (Figure 4D), indicating that the anomalies were clonal. As anticipated, comparisons between individuals showed much lower correlation.

Pi4ka Is Expressed in HSPC Budding from the HemEnd and in Adult Mouse Lineage-Negative Bone Marrow Cells

Next, we sought to evaluate the expression profile of Pi4ka in the hematopoietic compartment. Immunofluorescence staining in E9.5 mouse aortas captured HSPC, budding from HemEnd (CD31$^+$), expressing Pi4ka at the cell membrane (Figure S3A). Pi4ka was also expressed in a subset of CD45$^+$, lineage-cocktail-negative cells in the mouse adult bone marrow, but not in the associated vasculature (Cdh5$^+$) (Figures S3B and S3C). To confirm these findings, we performed qPCR for *Pi4ka* on sorted adult bone marrow cell populations, detecting elevated expression in Lin$^-$Sca1$^+$cKit$^+$ HSPCs compared with other progenitor populations and the Lin$^+$ cell fraction (Figure S3D). In addition, a microarray data from BloodChIP (Chacon et al., 2014) demonstrates the

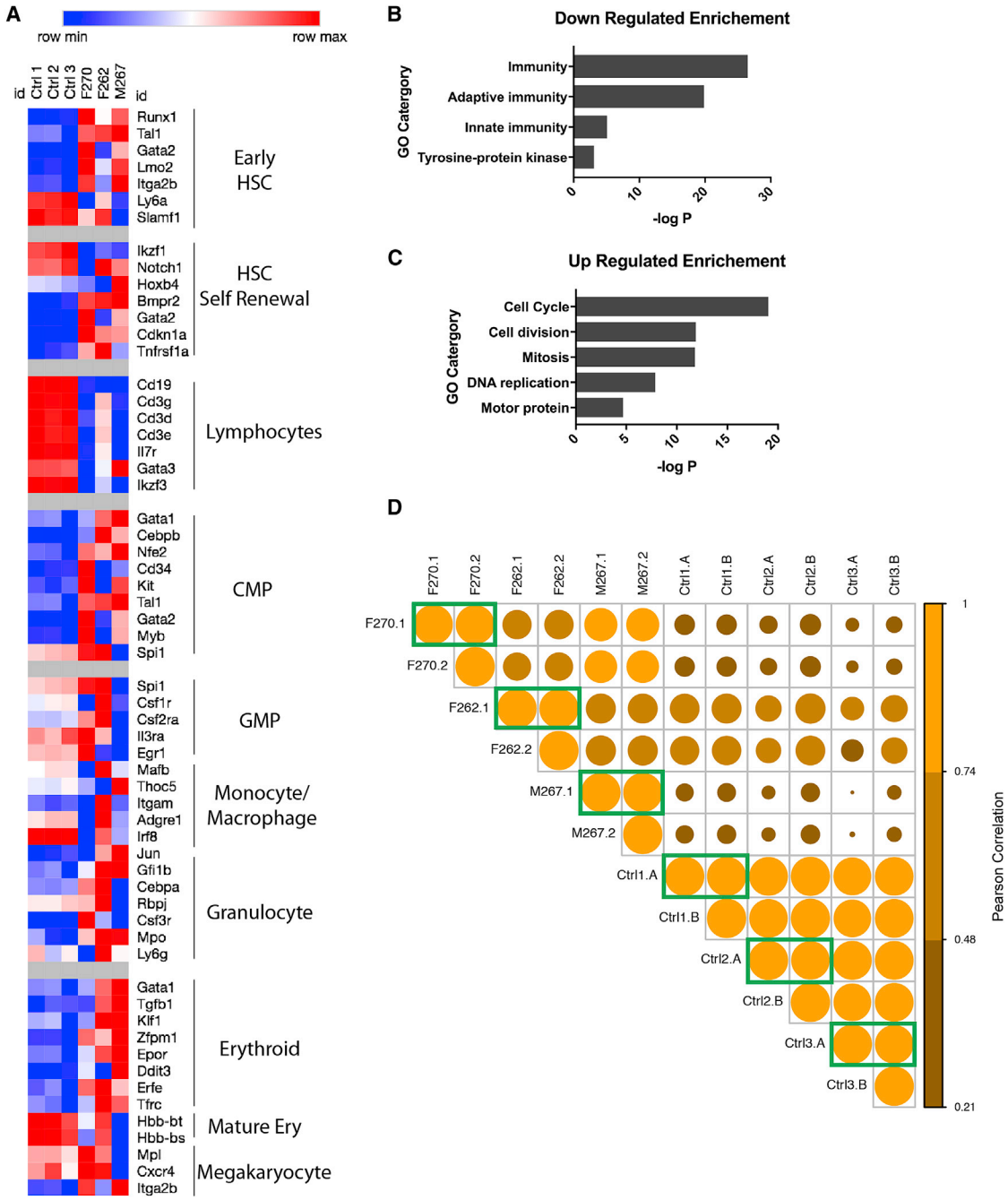

Figure 4. Molecular Characterization of Pi4ka Mutant Spleens

(A) Hematopoietic gene transcriptional signatures for the three Pi4ka affected mice compared to three controls.

(B and C) Gene Ontology categories enriched by genes downregulated (B) and upregulated (C) greater than 2-fold.

(D) Clonal analysis comparing transcript counts for hematopoietic genes (as in A) between two regions of spleen removed from the same mouse (green boxes). Pearson correlations are color coded and visualized by circle size.

See also Figure S3.

highest *PI4KA* expression in human HSC, multipotential progenitor (MPP), and megakarycocyte/erythrocyte progenitor (MEP) populations in addition to acute myeloid leukemia (AML) (Figure S3E).

Loss of *pi4kaa* Function in Zebrafish Inhibits Erythroid Differentiation

To further explore the biological relevance of Pi4ka in an independent system, we evaluated the role of zebrafish homolog *pi4kaa* in

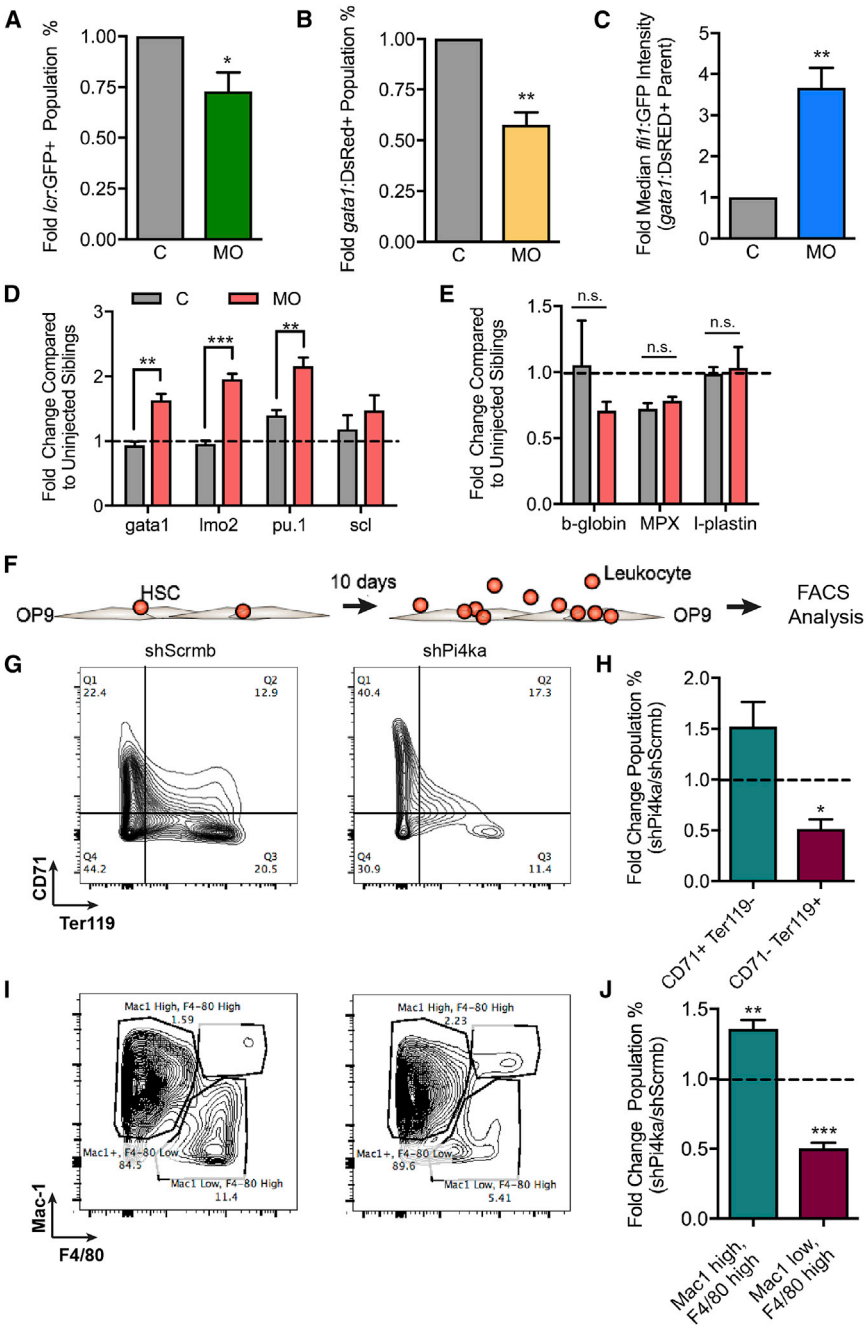

Figure 5. Loss of Pi4ka Decreases Erythroid Differentiation *In Vivo* and *In Vitro*

(A) Percent of LCR-GFP cells in MO fish compared with C for three independent experiments. For each data point in (A)–(C), >100 embryos were pooled and data are represented as mean ± SEM.

(B) Percent Gata1-DsRED cells in MO fish compared with C for four independent experiments.

(C) Graph of median Fli1:GFP intensity of the Gata1:DsRED parent population for four independent experiments.

(D) RNA expression in 24 hpf whole C and morpholino-injected embryos for gata1, lmo2, pu.1, and scl transcripts for three to four independent experiments. For each data point in (D) and (E), 20 embryos were pooled and data are represented as mean ± SEM.

(E) RNA expression in whole C and morpholino injected fish for b-globin, MPX, and l-plastin.

(F) Illustration of *in vitro* mouse HSPC differentiation on an OP9 stromal layer for 10 days.

(G) Three independent experiments in which shScrmb- and shPi4ka-infected HSPCs grown on OP9 stromal cells were probed for CD71 and Ter119 expression by flow cytometry.

(H) Quantification of three independent experiments plotted as the fold difference of shScrmb and shPi4ka.

(I) $Mac1^{+/-}$ (Mac1 high/low) and $F4/80^{+/-}$ (F4/80 high/low) expression and quantification in the same cells described in (G).

(J) Quantification of four independent experiments.

Bars indicate SEM. Student's t test and ANOVA were used to calculate significance between two groups (*$p \leq 0.05$; **$p \leq 0.01$; ***$p \leq 0.001$; ****$p \leq 0.0001$). See also Figure S4.

hematopoiesis. A splice inhibitory morpholino targeting the catalytic domain prevented splicing of *pi4kaa* exons 49 and 50 in a dose-dependent manner (Figure S4A). *o*-Dianisidine staining indicated lower hemoglobin content in the 48 hr post-fertilization (hpf) morphant embryos compared with controls (Figure S4B). To quantify differences in erythroid lineage cells, flow cytometry was performed on control and morpholino-treated *gata1*:DsRED (erythroid cells); *fli1*:GFP (endothelial and hematopoietic progenitor cells); or *lcr*:GFP (erythroid cells) embryos (≥100 embryos per biological replicate) at 48 hpf. Morphant (MO) animals were treated with an additional p53 morpholino to enhance embryo viability, whereas control (C) animals were treated with just the p53 morpholino. Due to its long half-life, DsRED measurement was equivalent to total erythroid lineage cells. *Pi4kaa* inhibition resulted in significantly less erythroid lineage cells in both fish lines (Figures 5A and 5B). *fli1*:GFP; *gata1*:DsRED fish were then used to assess the differentiation of erythroid lineage cells in MOs. In C embryos, a prominent *fli1:GFP;gata1:*DsRED double-positive population was observed at 24 hpf, characteristic of immature hematopoietic cells (Figure S4C). As development proceeded and cells differentiated, this population was decreased. By 48 hpf, *gata1*:DsRED cells had lost *fli1*:GFP expression in C embryos (Figure S4D). In contrast, the *fli1*:GFP;*gata1*:DsRED double-positive population was partially retained in *pi4kaa* MOs (~3.5 higher median *fli1*:GFP expression) (Figure 5C; Figure S4E).

We performed qPCR on whole *pi4kaa* MO and C embryos to assess markers of stem and mature blood cells. Indicators of

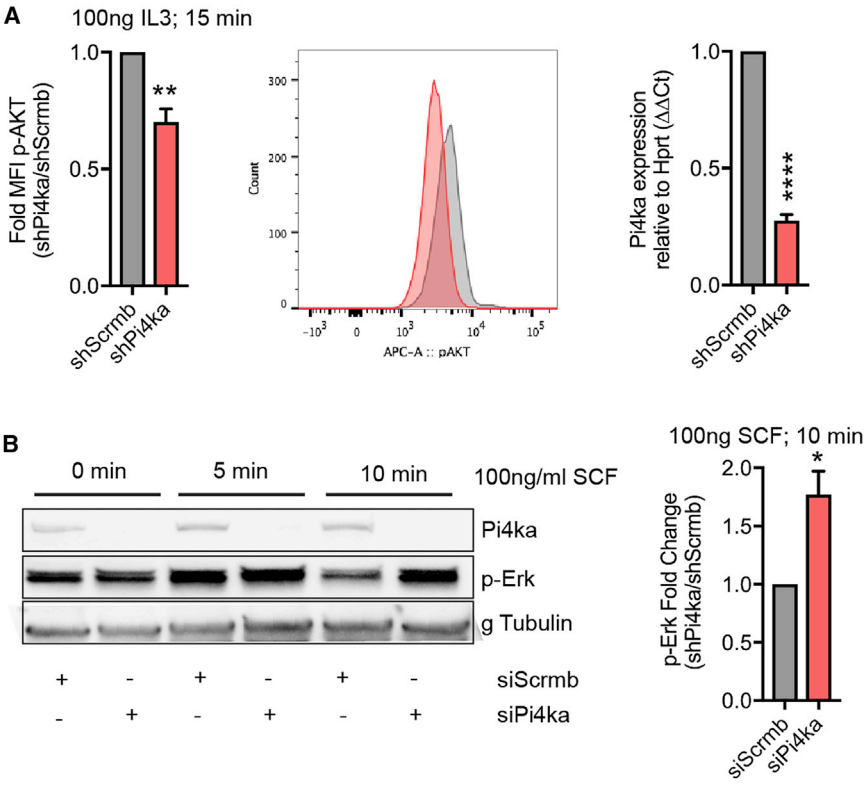

Figure 6. Loss of Pi4ka *In Vitro* Blunts Akt Signaling and Enhances ERK Signaling

(A) Phospho-flow cytometry on 32D cells treated with 100 ng/mL IL-3 for 15 min. Fold change in MFI ratio of shPi4ka:shScrmb. Representative FACS plot (middle). Quantification of Pi4ka knockdown in 32D cells by qPCR (right) (summary of three independent experiments ± SEM).

(B) HEK293 cells treated with siScrmb and siPi4ka were stimulated with 100 ng/mL SCF for 0, 5, and 10 min. Protein lysates were probed for Pi4ka, p-ERK, and gamma tubulin, as loading C. Quantification (right) (summary of three independent experiments ± SEM).

Student's t test and ANOVA were used to compare two conditions with statistical significance defined as *p ≤ 0.05; **p ≤ 0.01; ***p ≤ 0.001; ****p ≤ 0.0001. See also Figure S5.

hematopoiesis *gata1* (erythroid progenitor marker), *lmo2* (erythroid-myeloid progenitor marker), and *pu.1* (myeloid progenitor marker) were higher in MOs at 24 hpf (Figure 5D). While *beta-globin* was slightly lower than in Cs, the mature myeloid markers *mpx* and *l-plastin* were not affected in *pi4kaa* MOs (Figure 5E).

Pi4ka Knockdown in Mouse HSPC Impairs Progression of Mouse Erythro- and Myelopoiesis *In Vitro* in a Cell-Autonomous Manner

Given the evidence for a role in zebrafish erythropoiesis, we sought to determine the importance of Pi4ka in murine myelo- and erythropoiesis by evaluating HSPC differentiation *in vitro*. As the zebrafish experiments involved "whole-body" *pi4kaa* targeting, we sought to test whether Pi4ka loss functioned in a hematopoietic-cell-autonomous manner. We sorted adult mouse bone marrow HSPCs ($Lin^-cKit^+Sca1^+$), treated with either lentivirus (lenti)-small hairpin RNA against *Pi4ka* or scrambled sequence for 24 hr, washed to remove virus, and subsequently co-cultured on an OP9 stromal layer in the presence of cytokines (Figure 5F). After 10 days of culture, flow cytometry revealed significantly less $CD71^-$ (immature erythroid marker), $Ter119^+$ (mature eythroid marker) erythroid linage cells in cultures derived from shRNA for Pi4ka (shPi4ka)-treated HSPCs (Figures 5G and 5H). Similarly, an increase in $Mac1^+$ (Mac1 high), $F4/80^+$ (F4/80 high) cells with a complementary decrease in $Mac1^-$ (Mac1 low), $F4/80^+$ (F4/80 high) cells was observed in the shPi4ka-treated condition (Figures 5I and 5J), reflecting the phenotype seen in mouse F270 from the original screen.

A differentiation assay in the G1E-ER4 cell line also demonstrated an arrest in progressive differentiation (Ter119 level) with shPi4ka treatment (Figure S4F).

Akt and Erk Signaling Is Altered Downstream of Pik4a Knockdown *In Vitro*

To gain mechanistic clarity on pathways regulated downstream of Pi4ka, we explored the effect of loss of function on a panel of relevant signaling effectors. Pi4ka knockdown by lentiviral shRNA in 32D mouse myeloid lineage cells (Figure 6A, right) significantly increased phospho-ERK (p-Erk) and depressed interleukin-3 (IL-3)-induced p-Akt, as determined by western blot and flow cytometry (Figure 6A; Figure S5A). We validated the signaling effects in another cell type (HEK293), where *Pi4ka* small interfering RNA (siRNA) enhanced stem cell factor (SCF)-induced p-Erk levels (Figure 6B). Together, these results suggest that Pi4ka is important for regulating the balance between p-Akt and p-Erk signaling downstream of the cytokine receptors interleukin-3 receptor (IL-3R) and cKit.

Human PI4KAP2 Protein Lacks Kinase Activity and It Is Upregulated in Myelo- and Erythroleukemia Cell Lines

According to the COSMIC genome database, *PI4KA* mutations have been found in 363 unique human cancer samples, including somatic frameshift mutation p.T1995fs*4 in three lymphoid neoplasms (COSMIC Study COSU440) and many missense mutations, some occurring in primary and cell line leukemia. Interestingly, the human genome encodes pseudogenes, absent in mice, that could further affect PI4KA function. We hypothesized that human *PI4KAP2* (PI4KA pseudogene 2), which encodes an N-terminally truncated, kinase-domain-deleted version of the PI4KA protein (Figures 7A and 7B), could act in a dominant-negative manner. The BloodChIP database indicates that the *PI4KA* promoter is similarly primed by activation marks in both $CD34^+$ HSPCs and K562 eythroleukemia cells (Figure S6A), while the predicted *PI4KAP2* promoter has relatively

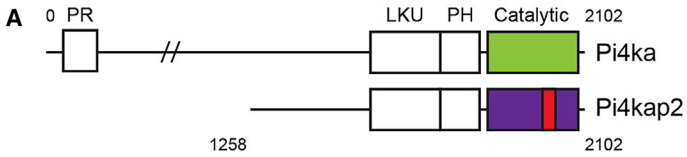

B

```
1       MTVEQKFGLFSAEIKEADPLAASEASQPKPCPPEVTPHYIWIDFLVQRFEIAKYCSSDQV  60
        MTVEQKFGLFSAEIKEADPLAASEASQPKPCPPEVTPHYIWIDFLVQRFEIAKYCSSDQV
1258    MTVEQKFGLFSAEIKEADPLAASEASQPKPCPPEVTPHYIWIDFLVQRFEIAKYCSSDQV  1317

61      EIFSSLLQRSMSLNIGRAKGSMNRHVAAIGPRFKLLTLGLSLLHADVVPNATIRNVLREK  120
        EIFSSLLQRSMSLNIG AKGSMNRHVAAIGPRFKLLTLGLSLLHADVVPNATIRNVLREK
1318    EIFSSLLQRSMSLNIGGAKGSMNRHVAAIGPRFKLLTLGLSLLHADVVPNATIRNVLREK  1377

121     IYSTAFDYFSCPPKFPTQGEKRLREDISIMIKFWTAMFSDKKYLTASQLVPP           172
        IYSTAFDYFSCPPKFPTQGEKRLREDISIMIKFWTAMFSDKKYLTASQLVPP
1378    IYSTAFDYFSCPPKFPTQGEKRLREDISIMIKFWTAMFSDKKYLTASQLVPP           1429

174     DIGDLLEQLVEENTGSLSGPAKDFYQREFDFFNKITNVSAIIKPYPKGDERKKACLSALS  233
        DIGDLL+QLVEE TGSLSGPAKDFYQREFDFFNKITNVSAIIKPYPKGDERKKACLSALS
1707    DIGDLLDQLVEEITGSLSGPAKDFYQREFDFFNKITNVSAIIKPYPKGDERKKACLSALS  1766

234     EVTVQPGCSLPSNPEAIVLDVDYKSGTPMQSAAKAPYLAKFKVKRCGVSELEKEGLRCRS  293
        EV VQPGC LPSNPEAIVLD+DYKSGTPMQSAAKAPYLAKFKVKRCGVSELEKEGLRCRS
1767    EVKVQPGCYLPSNPEAIVLDIDYKSGTPMQSAAKAPYLAKFKVKRCGVSELEKEGLRCRS  1826

294     DSEDECSTQEADGQKISWQAAIFKLGDDCRQDMLALQIIDLFKNIFQLVGLDLFVFPYRV  353
        DSEDECSTQEADGQKISWQAAIFK+GDDCRQDMLALQIIDLFKNIFQLVGLDLFVFPYRV
1827    DSEDECSTQEADGQKISWQAAIFKVGDDCRQDMLALQIIDLFKNIFQLVGLDLFVFPYRV  1886

354     VATAPGCGVIECIPDCTSRDQLGRQTDFGMYDYFTRQYGDESTLAFQQARYNFIRSMAAY  413
        VATAPGCGVIECIPDCTSRDQLGRQTDFGMYDYFTRQYGDESTLAFQQARYNFIRSMAAY
1887    VATAPGCGVIECIPDCTSRDQLGRQTDFGMYDYFTRQYGDESTLAFQQARYNFIRSMAAY  1946

414     SLLLFLLQIKDRHNGNIMLDKKGHIIHIDFGFMFESSPGGNLGWEPDIKLTDEMVMIMGG  473
        SLLLFLLQIKDRHNGNIMLDKKGHIIHIDFGFMFESSPGGNLGWEPDIKLTDEMVMIMGG
1947    SLLLFLLQIKDRHNGNIMLDKKGHIIHIDFGFMFESSPGGNLGWEPDIKLTDEMVMIMGG  2006

474     KMEATPFKWFMEMCVRGYLAVR------------------------------HRFSPNMT  503
        KMEATPFKWFMEMCVRGYLAVR                              HRFSPNMT
2007    KMEATPFKWFMEMCVRGYLAVRPYMDAVVSLVTLMLDTGLPCFRGQTIKLLKHRFSPNMT  2066

504     EREAANFIMKVIQSCFLSNRSRTYNMIQYYQNDIPY  539
        EREAANFIMKVIQSCFLSNRSRTY+MIQYYQNDIPY
2067    EREAANFIMKVIQSCFLSNRSRTYDMIQYYQNDIPY  2102
```

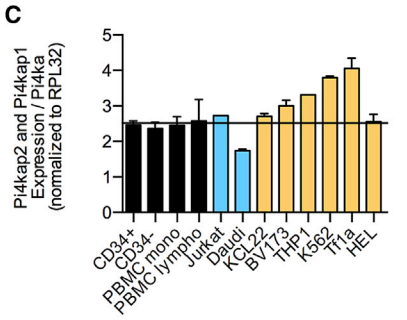

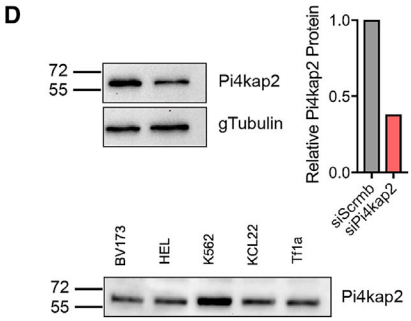

E

	Pi4kap2 vs. Ctrl	siPi4ka vs. siScrmb
Cyto-skeleton	Catenin b FAK (PTK2) LIMK1 PAK1	Cofilin 1 Paxillin 1 LIMK1 ITSN2
Src-family	FYN	FYN SRC
MAPK family	ERK1 (MAPK3) MEKK1 p38d MAPK	p38b MAPK p38g MAPK p38d MAPK
NFkappB	IkBa NFkappaB p50 NFkappaB p65	IKKa
RTK	KIT FGFR3 FRS2	KIT PDGFRa VEGFR2 (KDR)
Cell Cycle	AurKA (Aurora A)	CLK1 HCA59
JAK-Stat	STAT5A STAT5B	STAT5A JAK1
Intracellular Kinases	RSK1/2 p70 S6K	SIK3 (QSK) PKCq PRKACA
Adaptor	Gab1	
Lipase	PLCg2	

Figure 7. The Human *PI4KAP2* Gene Yields a Protein Product and Has Higher mRNA Expression Relative to *PI4KA* in Erythro- and Myelo-Leukemia Cell Lines

(A) Schematic comparing PI4KA and PI4KAP2 proteins. PI4KAP2 lacks the N-terminal domain and has a deletion in the kinase domain (red). PR, proline-rich domain; LKU, lipid kinase unique domain; PH, plekstrin homology domain.

(B) Alignment of PI4KA and PI4KAP2 amino acid sequences shows major homology starting at amino acid 1,258 of PI4KA, except for missing amino acids in the kinase domain of PI4KAP2.

(C) Ratio of mRNA expression of *PI4KAP2* and *PI4KAP1* compared with *PI4KA* in a panel of normal cord and peripheral blood cells (black), human lymphoid leukemia (blue), and myeloid leukemia (orange) cell lines.

(legend continued on next page)

higher activation marks in K562 (Figure S6B). Furthermore, K562 cells have both *PI4KA* and *PI4KAP2* promoter binding by the hematopoietic transcription factor Erg, while normal $CD34^+$ HSPCs do not (Figures S6C and S6D).

Given the apparent increased *PI4KAP2* promoter accessibility/priming and concomitant hematopoietic transcription factor binding in malignant cells, we assessed differential expression in myeloid leukemia, lymphoid leukemia, normal hematopoietic progenitor cells, and normal blood mononuclear cells (monocytes and lymphocytes) (Figure 7C). We designed primers to distinguish the *PI4KA* transcript (located in the region deleted in *PI4KAP2*) from the *PI4KAP1* and *PI4KAP2* transcripts (reverse primer spanning the region flanking the deleted kinase domain in *PI4KAP1/2*), although we were unable to distinguish between the two pseudogene transcripts. While *PI4KAP1/2* and *PI4KA* were similarly expressed in $CD34^+$ cord blood cells, peripheral blood mononuclear cells (PBMCs), and a T cell leukemia cell line, the ratio of *PI4KAP1/2* to *PI4KA* expression was generally increased in myelo- and erythroleukemia cell lines, consistent with the BloodChIP data. We confirmed expression of PI4KAP2 protein in the myelo- and erythroleukemia cell lines using an antibody validated through decreased signal after siRNA knockdown in HEK293 cells (Figure 7D). These results demonstrate that *PI4KAP2* codes for an expressed protein and is not a pseudogene, a conclusion further validated by fusing the cDNA sequence to a C-terminal hemagglutinin (HA)-tag. Both the exogenously expressed (HA-tagged) and endogenous protein were detected by western blot with a PI4KAP2 antibody (Figure S7A).

Given the lack of the kinase domain in PI4KAP2, we explored its potential role as an antagonistic regulator of PI4KA. As expected, PI4KAP2 protein purified from HEK293 cells using immuno-precipitation of the HA-tag displayed no *in vitro* kinase activity, in contrast to purified PI4KA protein (Figure S7B). We compared the impact of PI4KAP2 gain of function to PI4KA loss of function by probing an antibody microarray with lysates from HEK293 cells transfected with PI4KAP2 expression vector, C vector, siRNA against PI4KA, or C siRNA (Figures S7C and S7D). Protein categories affected by altering PI4KA signaling included cytoskeleton regulation, Src-family kinases, MAPK family, NFkappaB, receptor tyrosine kinases, cell cycle regulators, JAK-STAT signaling members, intracellular kinases, adaptors, and lipases (Figure 7E). Although there were some differences in the effects of PI4KAP2 expression and PI4KA knockdown, commonly affected proteins included: LIMK1 FYN, KIT, p38d MAPK, and STAT5A. The entire array can be found in Table S3.

DISCUSSION

Our results are consistent with literature reporting a pleiotropic requirement for Pi4ka in normal morphogenesis. In zebrafish, *pi4kaa* was shown to be necessary for pectoral fin development downstream of fibroblast growth factor receptor (FGFR) signaling through regulation of PI3K-Akt signaling (Ma et al., 2009). In *Drosophila*, it was shown to be required for smoothened activation during imaginal wing disc development (Yavari et al., 2010). Furthermore, global deletion of *Pi4ka* in adult mice uncovered its requirement for gastrointestinal stability (Bojjireddy et al., 2014; Vaillancourt et al., 2012). Our data add to this body of knowledge and implicate *Pi4ka* in hematopoiesis.

We postulate that *Pi4ka* is likely to regulate hematopoiesis in several ways in addition to its effect in Akt signaling. Pi4ka is a lipid kinase that phosphorylates the D4 position of the phosphatidyl-inositol ring (Minogue and Waugh, 2012). The resulting phosphatidyl-inositol, 4-phosphate (PIP4) provides a docking point for other proteins to bind to the inner leaflet of the plasma membrane (Balla et al., 2009). Once docked, additional lipid kinases can phosphorylate the ring at other positions, creating more complex phosphatidyl-inositols that can become substrates for phospholipases. Interestingly, phospholipase gamma 1 has been shown to have a role in primitive zebrafish hematopoiesis (Ma et al., 2007). In fact, we observe defects of the primitive erythroid lineage when we inhibit *pi4kaa* in our zebrafish model. Furthermore, oxysterol-binding proteins, which insert sterols into the plasma membrane (Villasmil et al., 2012), require PIP4 to dock. Oxysterols themselves can inhibit the proliferation of hematopoietic cell progenitors (Gregorio-King et al., 2002). Plasma membrane fluidity, as well as the specific constituency of lipids, influences cell-surface receptor signaling (Sunshine and Iruela-Arispe, 2017). Indeed, sterols have been shown to affect smoothened activation and hedgehog signaling, which are known to regulate HemEnd - HSCs (Crisan et al., 2016). Finally, there are early reports correlating changes in phosphatidyl-inositol lipid composition and hematopoietic cell proliferation and differentiation (Michell et al., 1990).

PI4KAP2, previously thought to not encode a functional protein, is the result of gene duplication in humans and does not exist in mice (Szentpetery et al., 2011). However, we demonstrated that this gene is not only transcribed, but also translated into a protein that has signaling consequences. Based on its lack of a kinase domain, we hypothesized that the PI4KAP2 protein could act in a dominant-negative fashion (similar to the effects of losing expression of PI4KA). The ratio of PI4KAP2 to PI4KA is higher in myeloid and erythroid cell lines compared with other cell types tested. Strikingly, the ERG transcription factor was documented to bind to the promoter region, specifically in malignant (K562) cells. One could speculate of a scenario in which higher levels of ERG (such as in Down syndrome) could enhance PI4KAP2 expression and deregulate the PI4KA pathway in the context of in utero leukemia development. Our findings indicate that PI4KAP2 overexpression or PI4KA knockdown induces similar alterations in MAPK, Srk-family kinases, and JAK-STAT signaling pathways. We also documented the effect of PI4KAP2

(D) Top: Validation of an antibody probing cells subjected to siRNA targeting PI4KAP2 and quantification. Bottom: Western blot showing endogenous PI4KAP2 in myeloid leukemia cell lines.

(E) Antibody array summary of proteins that change when lysates from cells overexpressing PI4KAP2 were compared with vector C (left) and of proteins that change when lysates from cells knocked down for PI4KA were compared with C cells (right). Proteins in common between the two comparisons are highlighted in red. See also Figures S6 and S7.

and PI4KA on proteins like FAK, PAK1, STAT5, and KIT, which are known leukemia drivers (Chatterjee et al., 2014). In addition, pi4kaa is known to regulate the PI3K-AKT pathway downstream of FGFR signaling (Ma et al., 2009). Our findings demonstrate similar effects in mouse 32D myeloid progenitor cells. FGFR1 signaling appears to be required for HSC repopulation, and increased expression of FGFR3 has been reported in $CD34^+$ myeloid leukemia cells (de Haan et al., 2003; Dvorak et al., 2003). In this study, PI4KAP2 overexpression altered FGFR3 protein levels as per findings in the antibody array.

In conclusion, this forward genetic screen supports the concept that mutations initiated at the hemogenic endothelium stage can carry consequences for the hematopoietic lineage. We identified Pi4ka as an important cell-autonomous regulator of hematopoiesis, which in turn pointed to PI4KAP2, found to be dysregulated in human myeloid and erythroid leukemia cell lines.

EXPERIMENTAL PROCEDURES

Mice

VEC-Cre; ROSA26-LacZ transgenic mice (Alva et al., 2006) were crossed to conditional ROSA26-LsL-SB transposase T2/Onc2 mice (Dupuy et al., 2005) to initiate mutagenesis in hemogenic endothelial cells starting at E9.5. VEC-Cre-negative and wild-type C57BL/6J mice were used as controls. iCdh5-Cre recombinase; Rosa26-TdTomato mouse femurs and tibia were flushed to isolate marrow strands (Lizama et al., 2015). Animal protocols were reviewed and approved by the University of California, Los Angeles (UCLA) Institutional Animal Care and use Committee (ARC#2005-223-33G).

Sequencing of Transposon Insertion Sites and Identification of Gene-Centric Common Insertion Sites (gCISs)

Genomic DNA from tumors was analyzed by ligation-mediated PCR (LM-PCR) to identify transposon integration sites, as previously described (Berquam-Vrieze et al., 2011). Briefly, genomic DNA was digested with either *Alu*I or *Nla*III restriction enzymes. Double-stranded adaptor oligonucleotides were ligated to free DNA ends, followed by two rounds of PCR with nested primers to specifically amplify transposon/genome junctions and add on sequences necessary for sequencing. Amplified junctions were purified and sequenced using Illumina HiSeq. Clonal insertion sites were defined and gene-centric CIS (gCIS) analyses were performed to identify candidate genes implicated in tumorigenesis, as previously described (Brett et al., 2011).

Hematology

Complete blood count (CBC) analysis was performed using a Hemavet machine (Drew Scientific). After RBC lysis, leukocytes were spun onto slides using a Shandon Cytospin 4 (Themo Fisher Scientific). Slides were stained with May-Grunwald and Giemsa stains (Sigma-Aldrich).

Immunohistochemistry

Paraformaldehyde-fixed, paraffin-embedded tissue sections were deparaffinized, subjected to heat-mediated antigen retrieval, blocked with normal serum, and stained with antibody against Pi4ka. Biotinylated anti-rabbit secondary antibody was followed by Avidin-Biotin Complex Elite and DAB Peroxidase Kit (Vector Laboratories). See antibodies in Supplemental Experimental Procedures. An Olympus DP73 camera and cellSens software were used to image non-fluorescent stains.

RNA Sequencing

RNA was purified using an RNeasy mini kit (QIAGEN), and libraries were prepared with a TruSeq polyA selection kit using 1 μg of RNA manually or a TruSeq stranded polyadenylation (poly-A) selection kit with 50 ng of RNA using the NeoPrep system (Illumina). Libraries were sequenced on a HiSeq 4000 system (Illumina). For the clonal analysis, we sequenced single-end 50 bp. For the cell-subtype expression analysis, we sequenced paired-end 100 bp.

Fish

Zebrafish lines were maintained in accordance with the UCLA Department of Laboratory Animal Medicine's Animal Research Committee guidelines. The following lines were used: Tg(gata1:DSRED; fli1:GFP), Tg(lcr:GFP) (Ganis et al., 2012), and wild-type AB fish. lcr:GFP fish were purchased from the UCLA Zebrafish Core Facility. All embryos were treated with 1× 1-phenul-2-thiorea (PTU) (to inhibit pigment formation) at 24 hpf. Eight pg or 12 pg of the splice-inhibitory *pi4kaa* morpholino was injected with 2 pg or 3 pg of p53 morpholino, respectively. Splicing efficiency was examined with previously published primers. See oligonucleotide sequences in Supplemental Experimental Procedures. *o*-Dianisidine stain was used to stain hemoglobin.

qPCR Transcriptional Analysis

RNA was isolated using RNeasy Mini and Micro kits (QIAGEN). Mouse tissue cDNA was made using a Superscript III system (Invitrogen). Zebrafish and human cDNA were generated with an iScript cDNA synthesis kit (BioRad). Twenty whole zebrafish per treatment were used for RNA isolation. Zebrafish, mouse, and human qPCR primers are listed in Supplemental Experimental Procedures. SYBR-Green-based qPCR (BioRad) was performed as previously described (Briot et al., 2014).

Cells

OP9 cells (a gift from the Mikkola Laboratory, UCLA) were cultured in alpha minimum essential medium (αMEM) with 2 mM L-glutamine, 1% pen-strep, 20% Hyclone (Thermo Fisher Scientific) fetal bovine serum (FBS). For OP9/leukocyte co-cultures, media was supplemented with 5 ng/mL thrombopoietin (TPO), 50 ng/mL SCF, 10 ng/mL FMS-like tyrosine kinase 3 ligand (Flt3L), 5 ng/mL interleukin-6 (IL-6), and 5 ng/mL IL-3 (Peprotech). 32D cells (CRL-11346 American Type Culture Collection [ATCC]) were cultured according to ATCC recommendations with 10 ng/mL IL-3. Lenti-X HEK293 cells (632180 Clonetech) were cultured in DMEM 10% FBS. G1E-ER4 cells (a gift from the Ganz Laboratory, UCLA) were cultured with tamoxifen according to Rylski et al. (2003). BV173, KCL22, and K562 cells (a gift from the Colicelli Laboratory, UCLA), Tf1a (ATCC CRL-2451) and HEL 92.1.7 (ATCC TIB-180) were all cultured according to ATCC recommendations.

Human PBMC and $CD34^+$ cord blood cells were purchased from the UCLA/Core Facility Research (CFAR) Virology Core Laboratory. Mononuclear cells were isolated using a Ficoll gradient. Monocytes (PBMC fraction adhering to a TC plate) and lymphocytes (non-adhered portion) were used for RNA. For cord blood, $CD34^+$ (positive selected) and $CD34^-$ (negative selected) blood cells were isolated using human Miltenyi MACS CD34 MicroBead Kit Ultra Pure and used for RNA.

Flow Cytometry and Cell Sorting

Flow cytometry was performed using BD Fortessa and LSRII machines (BD Biosciences). FACS was performed using BD Aria instruments. For RNA isolation of bone marrow subpopulations, Lin^+, HSC (Lin^-, $cKit^+$, $Sca1^+$, $CD34^-$), GMP (Lin^-, $cKit^+$, $Sca1^-$, $CD34^-$, $Fc\gamma R^+$), MEP (Lin^-, $cKit^+$, $Sca1^-$, $CD34^-$, $Fc\gamma R^-$), and CMP (Lin^-, $cKit^+$, $Sca1^-$, $CD34^+$, $Fc\gamma R^{low}$) cells were sorted from RBC-lysed bone marrow.

For OP9 cultures, HSC (Lin^-, $cKit^+$, $Sca1^+$) cells were sorted after lineage depletion of bone marrow using mouse lineage depletion kit and LS columns (Miltenyi). Mouse hematopoietic cell differentiation on OP9 cultures was assessed from a single-cell suspension generated from cultured cells using antibodies against CD45, Mac1 (CD11b), F4/80, Ter119, and CD71.

Zebrafish flow cytometry and sorting was based on *fli1*:GFP, *lcr*:GFP or *gata1*:DsRED fluorescent signal (n = 100 per treatment). Dechorionated embryos were digested with 5 μg/mL Liberase-TM (Roche) for 1 hr at 33°C as in Bertrand et al. (2007).

Molecular Cloning

The Pi4kap2 coding sequence was amplified from pDONR223-PI4KAP2 (23601 Addgene) using primers (Supplemental Experimental Procedures) that introduced an HA-tag at the 3′ end and flanked the fragment with PstI

and *Age*I restriction enzyme sequences. The fragment was ligated into the pJet cloning vector using CloneJET kit instructions (K1231 Thermo Fisher Scientific) and amplified in Stbl3 bacteria (C737303 Thermo Fisher Scientific). The pLV-Ef1a-MCS-IRES-RFP-puro plasmid and the Pi4kap2HA-pJet vector were linearized with PstI and *Age*I. The Pi4kap2-HA fragment was gel purified and ligated into the pLV vector using T4 ligase. For the shRNA vector purchased from Origene (TL510615), the MND-GFP cassette (a gift from the Kohn Laboratory) was used to replace the CMV-GFP reporter.

Lenti shRNA Transduction

Pi4ka or scrambled shRNA plasmids along with VSG-G and Δ8.2 packaging plasmids were transfected into 293T cells using Lipofectamine 2000 (LifeTechnologies). Virus was collected and concentrated by centrifugation. For primary HSPCs, high concentration virus was used to doubly infect cells using Retronectin-coated (Clontech) plates (40 μg/mL) after an overnight pre-stimulation in serum-free StemSPAN (StemCell Technologies, Inc.) or StemMACS (Miltenyi) supplemented with four times the cytokine concentration used in OP9 co-culture over the course of 24 hr before being washed and moved to OP9 stromal cells. For 32D and G1E-ER4 cells, the same virus was used to doubly infect cells using Retronectin-coated plates as above for 24 hr in the presence of culture medium.

Cell Transfection

For siRNA studies, HEK293 cells were treated with 60 pmol non-targeted (4390843 Invitrogen), Pi4ka-targeted siRNA (4392420 ID:s224264, Invitrogen) or Pi4kap2-targeted siRNA (4390771 ID: n310610) in the presence of Lipofectamine RNAi Max (Invitrogen) for two days. Similarly, for overexpression of Pi4kap2, cells were treated with 3 μg of pLV-Ef1a-Pi4kap2-HA-RFP in the presence of Lipofectamine2000 (Invitrogen) for two days.

Western Blot

32D cells and HEK293 cells were lysed in modified radioimmunoprecipitation assay (mRIPA) buffer (50 mM Tris, pH 7.4, 1% NP-40, 0.25% sodium deoxycholate, 1 mM EDTA, 0.15M NaCl, and 10mM beta-glycerophosphate) in the presence of 200 μM Na_3VO_4 and protease inhibitor cocktail (11873580001, Sigma). Lysates were run on 4%–20% gradient acrylamide gels (BioRad) and transferred to nitrocellulose membranes. See antibodies in Supplemental Experimental Procedures.

Antibody Array

Cell lines expressing Ef1a-Pi4kap2-HA-RFP, Ef1a-RFP empty vector, non-targeted siRNA, or Pi4ka-targeted RNA were lysed in protein lysis buffer (5 mM EDTA, 2 mM EGTA, 20 mM 3-(N-morpholino)propanesulfonic acid (MOPS), pH 7.0, 20 mM NaF, 20 mM $Na_4P_20_7$, 1 mM Na_3VO_4, 60 mM beta-glycerophosphate, 50 nM phenylarsine oxide, 1% Triton X-100) containing protease inhibitor cocktail and phosphatase inhibitors. Samples were sonicated and then centrifuged for 30 min at 14,000 × *g*. Protein was quantified and pooled at equal concentrations. Lysates were then probed using the Kinexus KAM-900P array (Kinexus Bioinformatics Corporation), which contains 613 phospho-site-specific antibodies and 265 pan-specific antibodies (targeting 878 cell signaling proteins).

Statistical Analysis

For every dataset, it was first determined wither parametric or non-parametric analysis was appropriate and the use of either Student's t test or Mann Whitney to assess significance. Log-rank test was used for survival curve statistics. Paired Student's t test and one-way ANOVA were used to assess the significance of transcriptional differences between sorted hematopoietic sub-populations with the null assumption that they were the same. Paired Student's t test was used to assess significance between experimental and C conditions for zebrafish and OP9 co-culture experiments. Unpaired Student's t test was used for western blot and MFIR calculations. Statistical analyses were performed in Prism 7.0 according to the manufacturer's recommendations (GraphPad Software) (*$p \leq 0.05$; **$p \leq 0.01$; ***$p \leq 0.001$; ****$p \leq 0.0001$).

DATA AND SOFTWARE AVAILABILITY

The accession number for all datasets reported in this paper is GEO: GSE108355.

SUPPLEMENTAL INFORMATION

Supplemental Information includes Supplemental Experimental Procedures, seven figures, and three tables and can be found with this article online at https://doi.org/10.1016/j.celrep.2018.01.017.

ACKNOWLEDGMENTS

The authors wish to thank Ms. Michelle Steel, Dr. Vincenzo Calvanese, Ms. Felicia Codrea, Ms. Jessica Scholes, Ms. Valerie Rezek, Ms. Deborah Anisman-Posner, and Mr. Ha Neul Lee for valuable technical assistance; Drs. Don Kohn and Hanna Mikkola for guidance; the UCLA Broad Stem Cell Institute Flow Cytometry Core; the UCLA Tissue Procurement Core Laboratory; the UCLA Zebrafish Core Facility; the UCLA Vector Core supported by CURE/P30 DK041301; and the UCLA/CFAR Virology Core Laboratory (grant 5P30 AI028697). This work was supported by NIH grant CA197943 to M.L.I.-A. and N.R.S.A. (T32 HL69766) and a United Negro College Fund (UNCF)/Merck Graduate Science Research Dissertation Fellowship to S.Z (grant 20145117).

AUTHOR CONTRIBUTIONS

S.Z. designed and performed the experiments, analyzed the data, and wrote the paper. J.D.R. designed and performed the experiments, analyzed the data, and assisted in manuscript preparation. A.M.C. designed and performed the experiments and analyzed the data. G.E.H. performed the experiments and analyzed the data. K.H., M.M., T.S., K.C.W., and G.H. performed the experiments. J.-N.C. and A.J.D. provided critical reagents and guidance. L.I.-A. designed the study, analyzed the data, and wrote the paper.

DECLARATION OF INTERESTS

We have no conflicts of interest to report.

Received: May 30, 2017
Revised: November 5, 2017
Accepted: January 5, 2018
Published: January 30, 2018

REFERENCES

Alva, J.A., Zovein, A.C., Monvoisin, A., Murphy, T., Salazar, A., Harvey, N.L., Carmeliet, P., and Iruela-Arispe, M.L. (2006). VE-Cadherin-Cre-recombinase transgenic mouse: a tool for lineage analysis and gene deletion in endothelial cells. Dev. Dyn. *235*, 759–767.

Athanasiou, M., Mavrothalassitis, G., Sun-Hoffman, L., and Blair, D.G. (2000). FLI-1 is a suppressor of erythroid differentiation in human hematopoietic cells. Leukemia *14*, 439–445.

Balla, T., Szentpetery, Z., and Kim, Y.J. (2009). Phosphoinositide signaling: new tools and insights. Physiology (Bethesda) *24*, 231–244.

Bard-Chapeau, E.A., Nguyen, A.-T., Rust, A.G., Sayadi, A., Lee, P., Chua, B.Q., New, L.-S., de Jong, J., Ward, J.M., Chin, C.K.Y., et al. (2014). Transposon mutagenesis identifies genes driving hepatocellular carcinoma in a chronic hepatitis B mouse model. Nat. Genet. *46*, 24–32.

Been, R.A., Linden, M.A., Hager, C.J., DeCoursin, K.J., Abrahante, J.E., Landman, S.R., Steinbach, M., Sarver, A.L., Largaespada, D.A., and Starr, T.K. (2014). Genetic signature of histiocytic sarcoma revealed by a sleeping beauty transposon genetic screen in mice. PLoS ONE *9*, e97280.

Berquam-Vrieze, K.E., Nannapaneni, K., Brett, B.T., Holmfeldt, L., Ma, J., Zagorodna, O., Jenkins, N.A., Copeland, N.G., Meyerholz, D.K., Knudson, C.M.,

et al. (2011). Cell of origin strongly influences genetic selection in a mouse model of T-ALL. Blood *118*, 4646–4656.

Bertrand, J.Y., Kim, A.D., Violette, E.P., Stachura, D.L., Cisson, J.L., and Traver, D. (2007). Definitive hematopoiesis initiates through a committed erythromyeloid progenitor in the zebrafish embryo. Development *134*, 4147–4156.

Bojjireddy, N., Botyanszki, J., Hammond, G., Creech, D., Peterson, R., Kemp, D.C., Snead, M., Brown, R., Morrison, A., Wilson, S., et al. (2014). Pharmacological and genetic targeting of pPI4KA reveals its important role in maintaining plasma membrane PtdIns4p and PtdIns(4,5)p2 levels. J. Biol. Chem. *289*, 6120–6132.

Brett, B.T., Berquam-Vrieze, K.E., Nannapaneni, K., Huang, J., Scheetz, T.E., and Dupuy, A.J. (2011). Novel molecular and computational methods improve the accuracy of insertion site analysis in Sleeping Beauty-induced tumors. PLoS ONE *6*, e24668.

Briot, A., Jaroszewicz, A., Warren, C.M., Lu, J., Touma, M., Rudat, C., Hofmann, J.J., Airik, R., Weinmaster, G., Lyons, K., et al. (2014). Repression of Sox9 by Jag1 is continuously required to suppress the default chondrogenic fate of vascular smooth muscle cells. Dev. Cell *31*, 707–721.

Chacon, D., Beck, D., Perera, D., Wong, J.W.H., and Pimanda, J.E. (2014). BloodChIP: a database of comparative genome-wide transcription factor binding profiles in human blood cells. Nucleic Acids Res. *42*, D172–D177.

Challen, G.A., Boles, N.C., Chambers, S.M., and Goodell, M.A. (2010). Distinct hematopoietic stem cell subtypes are differentially regulated by TGF-beta1. Cell Stem Cell *6*, 265–278.

Chatterjee, A., Ghosh, J., Ramdas, B., Mali, R.S., Martin, H., Kobayashi, M., Vemula, S., Canela, V.H., Waskow, E.R., Visconte, V., et al. (2014). Regulation of Stat5 by FAK and PAK1 in oncogenic FLT3- and KIT-driven leukemogenesis. Cell Rep. *9*, 1333–1348.

Chen, M.J., Li, Y., De Obaldia, M.E., Yang, Q., Yzaguirre, A.D., Yamada-Inagawa, T., Vink, C.S., Bhandoola, A., Dzierzak, E., and Speck, N.A. (2011). Erythroid/myeloid progenitors and hematopoietic stem cells originate from distinct populations of endothelial cells. Cell Stem Cell *9*, 541–552.

Clements, W.K., and Traver, D. (2013). Signalling pathways that control vertebrate haematopoietic stem cell specification. Nat. Rev. Immunol. *13*, 336–348.

Copeland, N.G., and Jenkins, N.A. (2010). Harnessing transposons for cancer gene discovery. Nat. Rev. Cancer *10*, 696–706.

Crisan, M., Kartalaei, P.S., Vink, C.S., Yamada-Inagawa, T., Bollerot, K., van IJcken, W., van der Linden, R., de Sousa Lopes, S.M., Monteiro, R., Mummery, C., and Dzierzak, E. (2015). BMP signalling differentially regulates distinct haematopoietic stem cell types. Nat. Commun. *6*, 8040.

Crisan, M., Solaimani Kartalaei, P., Neagu, A., Karkanpouna, S., Yamada-Inagawa, T., Purini, C., Vink, C.S., van der Linden, R., van Ijcken, W., Chuva de Sousa Lopes, S.M., et al. (2016). BMP and Hedgehog regulate distinct AGM hematopoietic stem cells ex vivo. Stem Cell Reports *6*, 383–395.

de Haan, G., Weersing, E., Dontje, B., van Os, R., Bystrykh, L.V., Vellenga, E., and Miller, G. (2003). In vitro generation of long-term repopulating hematopoietic stem cells by fibroblast growth factor-1. Dev. Cell *4*, 241–251.

Dupuy, A.J., Akagi, K., Largaespada, D.A., Copeland, N.G., and Jenkins, N.A. (2005). Mammalian mutagenesis using a highly mobile somatic Sleeping Beauty transposon system. Nature *436*, 221–226.

Dupuy, A.J., Rogers, L.M., Kim, J., Nannapaneni, K., Starr, T.K., Liu, P., Largaespada, D.A., Scheetz, T.E., Jenkins, N.A., and Copeland, N.G. (2009). A modified sleeping beauty transposon system that can be used to model a wide variety of human cancers in mice. Cancer Res. *69*, 8150–8156.

Dvorak, P., Dvorakova, D., Doubek, M., Faitova, J., Pacholikova, J., Hampl, A., and Mayer, J. (2003). Increased expression of fibroblast growth factor receptor 3 in CD34+ BCR-ABL+ cells from patients with chronic myeloid leukemia. Leukemia *17*, 2418–2425.

Dzierzak, E., and de Pater, E. (2016). Regulation of blood stem cell development. Curr. Top. Dev. Biol. *118*, 1–20.

Eliades, A., Wareing, S., Marinopoulou, E., Fadlullah, M.Z.H., Patel, R., Grabarek, J.B., Plusa, B., Lacaud, G., and Kouskoff, V. (2016). The hemogenic competence of endothelial progenitors is restricted by Runx1 silencing during embryonic development. Cell Rep. *15*, 2185–2199.

Ganis, J.J., Hsia, N., Trompouki, E., de Jong, J.L.O., DiBiase, A., Lambert, J.S., Jia, Z., Sabo, P.J., Weaver, M., Sandstrom, R., et al. (2012). Zebrafish globin switching occurs in two developmental stages and is controlled by the LCR. Dev. Biol. *366*, 185–194.

Gregorio-King, C.C., Collier, F.M., Bolton, K.A., Ferguson, M., Hosking, J.B., Collier, G.R., and Kirkland, M.A. (2002). Effect of oxysterols on hematopoietic progenitor cells. Exp. Hematol. *30*, 670–678.

Guibentif, C., Rönn, R.E., Böiers, C., Lang, S., Saxena, S., Soneji, S., Enver, T., Karlsson, G., and Woods, N.-B. (2017). Single-cell analysis identifies distinct stages of human endothelial-to-hematopoietic transition. Cell Rep. *19*, 10–19.

Huang, H., Yu, M., Akie, T.E., Moran, T.B., Woo, A.J., Tu, N., Waldon, Z., Lin, Y.Y., Steen, H., and Cantor, A.B. (2009). Differentiation-dependent interactions between RUNX-1 and FLI-1 during megakaryocyte development. Mol. Cell. Biol. *29*, 4103–4115.

Keng, V.W., Villanueva, A., Chiang, D.Y., Dupuy, A.J., Ryan, B.J., Matise, I., Silverstein, K.A.T., Sarver, A., Starr, T.K., Akagi, K., et al. (2009). A conditional transposon-based insertional mutagenesis screen for genes associated with mouse hepatocellular carcinoma. Nat. Biotechnol. *27*, 264–274.

Lizama, C.O., Hawkins, J.S., Schmitt, C.E., Bos, F.L., Zape, J.P., Cautivo, K.M., Borges Pinto, H., Rhyner, A.M., Yu, H., Donohoe, M.E., et al. (2015). Repression of arterial genes in hemogenic endothelium is sufficient for haematopoietic fate acquisition. Nat. Commun. *6*, 7739.

Ma, A.C.H., Liang, R., and Leung, A.Y.H. (2007). The role of phospholipase C gamma 1 in primitive hematopoiesis during zebrafish development. Exp. Hematol. *35*, 368–373.

Ma, H., Blake, T., Chitnis, A., Liu, P., and Balla, T. (2009). Crucial role of phosphatidylinositol 4-kinase IIIalpha in development of zebrafish pectoral fin is linked to phosphoinositide 3-kinase and FGF signaling. J. Cell Sci. *122*, 4303–4310.

Manabe, N., Kubota, Y., Kitanaka, A., Ohnishi, H., Taminato, T., and Tanaka, T. (2006). Src transduces signaling via growth hormone (GH)-activated GH receptor (GHR) tyrosine-phosphorylating GHR and STAT5 in human leukemia cells. Leuk. Res. *30*, 1391–1398.

Michell, R.H., Conroy, L.A., Finney, M., French, P.J., Brown, G., Creba, J.A., Bunce, C.M., and Lord, J.M. (1990). Inositol lipids and phosphates in the regulation of the growth and differentiation of haemopoietic and other cells. Philos. Trans. R. Soc. Lond. B Biol. Sci. *327*, 193–207.

Minogue, S., and Waugh, M.G. (2012). The phosphatidylinositol 4-kinases: don't call it a comeback. Subcell. Biochem. *58*, 1–24.

Moriarity, B.S., and Largaespada, D.A. (2015). Sleeping Beauty transposon insertional mutagenesis based mouse models for cancer gene discovery. Curr. Opin. Genet. Dev. *30*, 66–72.

Oki, T., Kitaura, J., Watanabe-Okochi, N., Nishimura, K., Maehara, A., Uchida, T., Komeno, Y., Nakahara, F., Harada, Y., Sonoki, T., et al. (2011). Aberrant expression of RasGRP1 cooperates with gain-of-function NOTCH1 mutations in T-cell leukemogenesis. Leukemia *26*, 1038–1045.

Orkin, S.H., and Zon, L.I. (2008). Hematopoiesis: an evolving paradigm for stem cell biology. Cell *132*, 631–644.

Rasmussen, M.H., Wang, B., Wabl, M., Nielsen, A.L., and Pedersen, F.S. (2009). Activation of alternative Jdp2 promoters and functional protein isoforms in T-cell lymphomas by retroviral insertion mutagenesis. Nucleic Acids Res. *37*, 4657–4671.

Riordan, J.D., Drury, L.J., Smith, R.P., Brett, B.T., Rogers, L.M., Scheetz, T.E., and Dupuy, A.J. (2014). Sequencing methods and datasets to improve functional interpretation of sleeping beauty mutagenesis screens. BMC Genomics *15*, 1150.

Rylski, M., Welch, J.J., Chen, Y.-Y., Letting, D.L., Diehl, J.A., Chodosh, L.A., Blobel, G.A., and Weiss, M.J. (2003). GATA-1-mediated proliferation arrest during erythroid maturation. Mol. Cell. Biol. *23*, 5031–5042.

Sunshine, H., and Iruela-Arispe, M.L. (2017). Membrane lipids and cell signaling. Curr. Opin. Lipidol. *28*, 408–413.

Szentpetery, Z., Szakacs, G., Bojjireddy, N., Tai, A.W., and Balla, T. (2011). Genetic and functional studies of phosphatidyl-inositol 4-kinase type IIIα. Biochim. Biophys. Acta. *1811*, 476–483.

Vaillancourt, F.H., Brault, M., Pilote, L., Uyttersprot, N., Gaillard, E.T., Stoltz, J.H., Knight, B.L., Pantages, L., McFarland, M., Breitfelder, S., et al. (2012). Evaluation of phosphatidylinositol-4-kinase IIIα as a hepatitis C virus drug target. J. Virol. *86*, 11595–11607.

Villasmil, M.L., Bankaitis, V.A., and Mousley, C.J. (2012). The oxysterol-binding protein superfamily: new concepts and old proteins. Biochem. Soc. Trans. *40*, 469–473.

Yavari, A., Nagaraj, R., Owusu-Ansah, E., Folick, A., Ngo, K., Hillman, T., Call, G., Rohatgi, R., Scott, M.P., and Banerjee, U. (2010). Role of lipid metabolism in smoothened derepression in hedgehog signaling. Dev. Cell *19*, 54–65.

Zhu, J., and Emerson, S.G. (2002). Hematopoietic cytokines, transcription factors and lineage commitment. Oncogene *21*, 3295–3313.

Zochodne, B., Truong, A.H., Stetler, K., Higgins, R.R., Howard, J., Dumont, D., Berger, S.A., and Ben-David, Y. (2000). Epo regulates erythroid proliferation and differentiation through distinct signaling pathways: implication for erythropoiesis and Friend virus-induced erythroleukemia. Oncogene *19*, 2296–2304.

Cell Reports, Volume *22*

Supplemental Information

A Forward Genetic Screen Targeting the Endothelium Reveals a Regulatory Role for the Lipid Kinase Pi4ka in Myelo- and Erythropoiesis

Safiyyah Ziyad, Jesse D. Riordan, Ann M. Cavanaugh, Trent Su, Gloria E. Hernandez, Georg Hilfenhaus, Marco Morselli, Kristine Huynh, Kevin Wang, Jau-Nian Chen, Adam J. Dupuy, and M. Luisa Iruela-Arispe

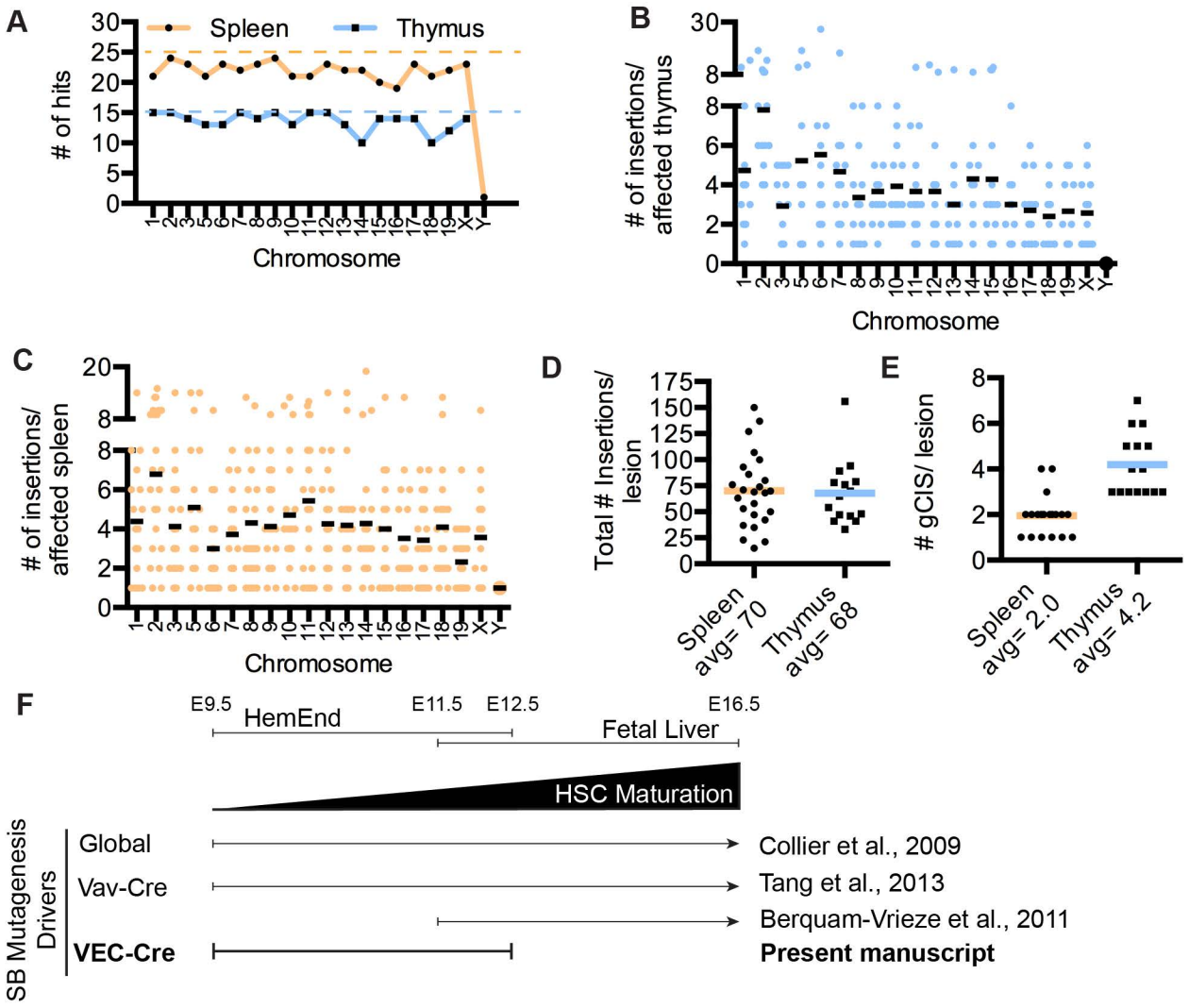

Figure S1: Transposition is unbiased, Related to Figure 2

(A) Plotting the number of hits per chromosome shows that every chromosome is hit by the transposon in both enlarged spleen and thymus tissues. Dotted lines indicate the total number of either spleen and thymus and shows that the majority of these lesions have insertions in all of the chromosomes. (B,C) The total number of insertions per spleen or thymus per chromosome shows there is little influence of chromosome size on number of insertions. Chromosome 4, the transposon donor chromosome, was removed from analysis due to preponderance of local hopping. (D) The average number of insertions per spleen is equal to that of the thymus, yet the average number of gCIS per spleen or thymus is higher in the thymus (E). (F) VEC-Cre initiates mutagenesis during a narrow time window (E9.5-12.5) This is distinct from other Cre initiated and global mutagenesis screens.

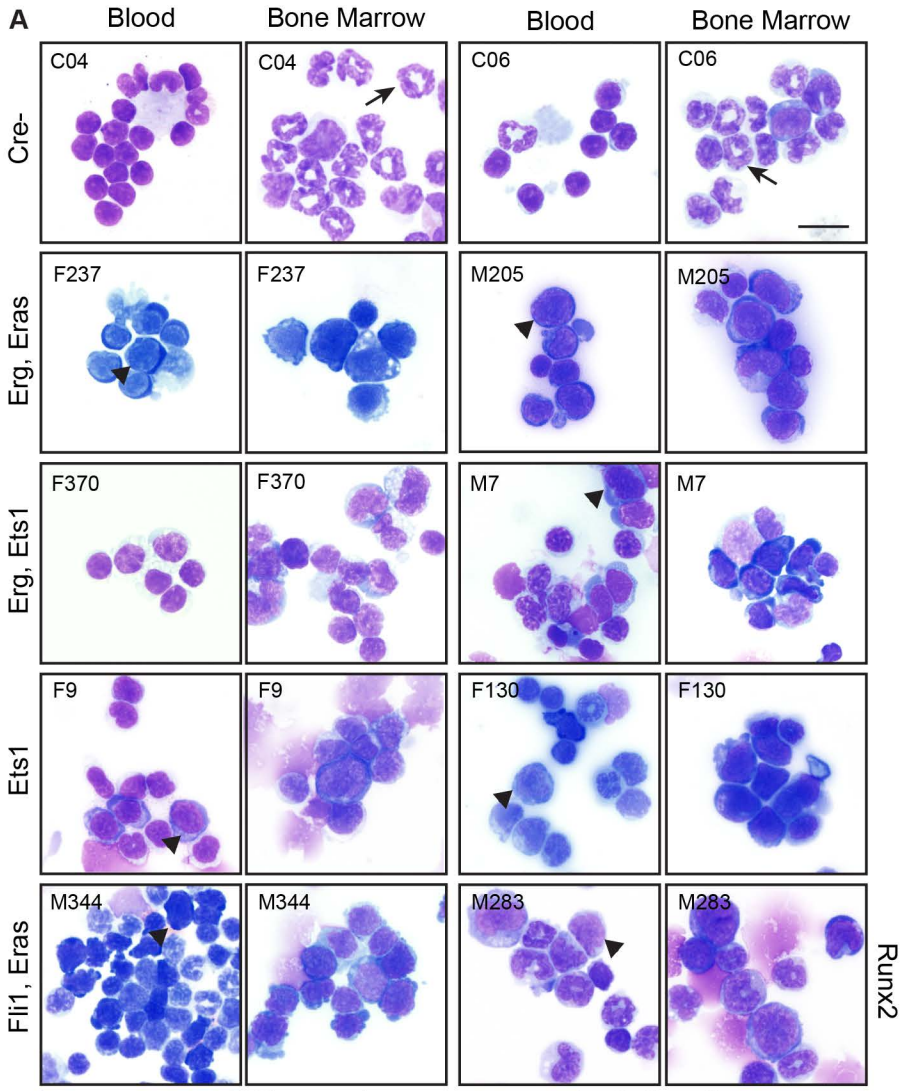

B

	M6	M332	M205	F237	F369	M344	F340	F370	M7	F9	F280	F130	M267	M278	M208	F262	M283	F270
Spleen Size	3	3	3	3	3	3	2	3	3	2	2	2	3	1	3	3	3	1
BM Blast-like	Y	Y	Y	Y	Y	Y	Y	Y	Y	Y	L	Y	Y	N/A	N/A	Y	Y	N/A
BM Neutrophils	L	L	L	L	N	N	L	N	N	N	Y	L	N	N	N/A	L	L	N/A
Blood Blast-like	Y	Y	Y	Y	Y	Y	Y	Y	Y	Y	N/A	Y	N	N	N/A	N	N	Y

Figure S2: Blast-like cells in peripheral blood and bone marrow are associated with gCIS, Related to Figure 2
(A) Mutations in certain gCIS genes were associated with a prevalence of large blast-like immature cells with high nucleus to cytoplasmic ratio in the blood and bone marrow of affected mice. A significant decrease in polymorpho-nuclear cells was observed in the bone marrow of affected animals (scale= 15μm). (arrow= polymorpho-nuclear cell, arrowhead= blast cell) (B) The majority of detected mutation patterns from Figure 2F were associated with very large spleens (3> 800mg, 800>2>500mg, 1<500mg), blast-like cells in the blood, and reduced polymorpho-nuclear cells in the bone marrow of affected animals (each column). M=male, F= female; numbers indicate individual ID number for each mouse.

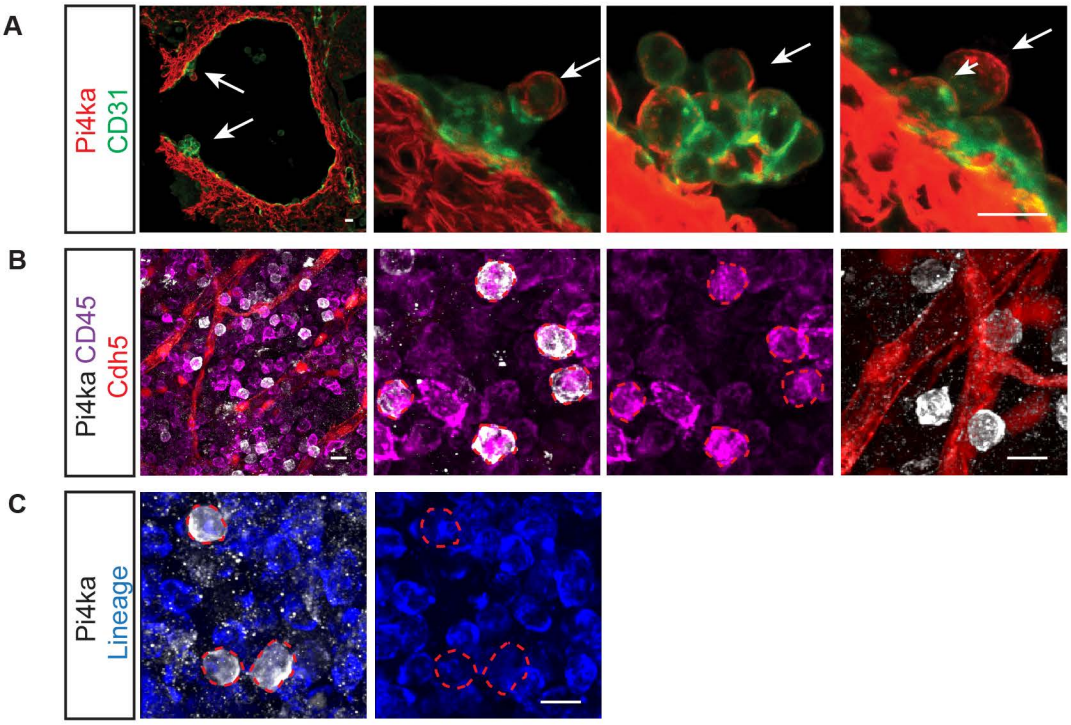

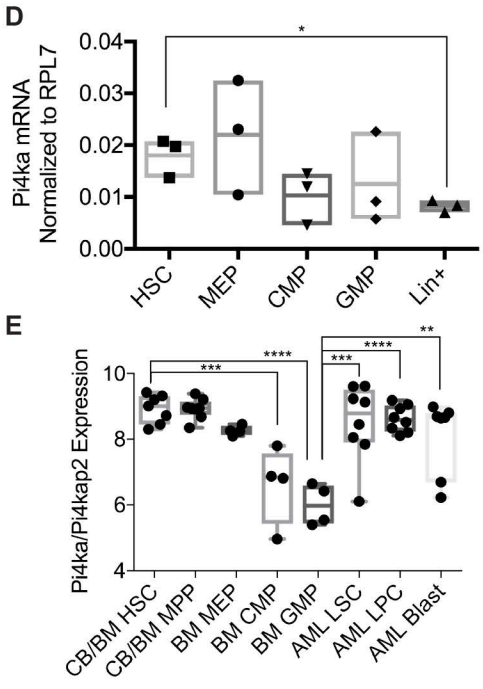

Figure S3: Pi4ka expression in HSPC budding from HemEnd and in adult lineage negative bone marrow cells, Related to Figure 4

(A) Pi4ka (red) was observed in the subaortic mesenchyme, but was also found in the membrane of the budding HSPC (CD31 positive, green) from hemogenic E9.5 aorta. (B) Pi4ka (white), CD45 (magenta), and Cdh5-Tomato vasculature (red) immunofluorescence of adult mouse bone marrow. (C) Immunofluorescence of Cdh5-Tomato adult mouse bone marrow with Pi4ka (white) and lineage cocktail (blue). (A-C, scale = 10μm) (D) Expression of Pi4ka was higher in HSC (Lin-cKit+Sca1+) and myeloid/erythroid populations of mouse adult marrow when compared to Lin+ differentiated hematopoietic cells. (E) Pi4ka/Pi4kap2 mRNA expression is higher in HSC and myeloid/erythroid lineage human populations in human bone marrow as well as in AML (BloodChIP) Graphs represent mean ± SEM comparisons done by t-test (D) or ANOVA (E). Individual samples are indicated by filled dots.

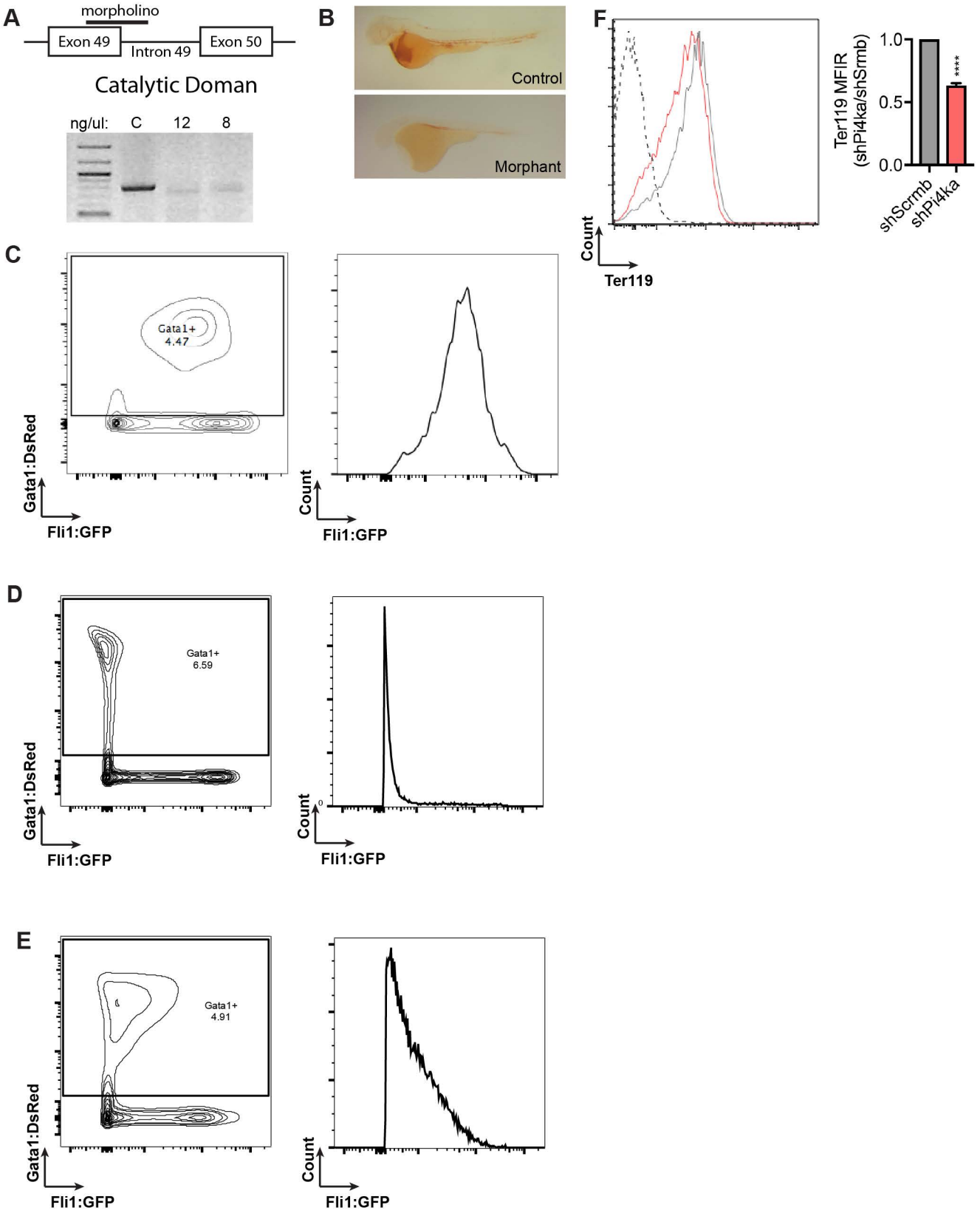

Figure S4: Loss of Pi4ka decreases erythroid differentiation in vivo and in vitro, Related to Figure 5
(A) Morpholino targeted splicing in the catalytic domain. PCR to assess splicing efficiency. (B) O-dianisidine marking hemoglobin in control and morphant fish. (C) 24 hpf control injected embryos were subjected to flow cytometry and Gata1:DsRED was plotted against Fli1:GFP (left). Histogram of Gata1:DsRED+ cells as a subpopulation of Fli1:GFP cell population. (D,E) Identical gating performed on 48 hour control (top) and morphant embryos (bottom). (F) G1E-ER4 cell differentiation in the presence of 4-hydroxytamoxifen (solid line) or ethanol control (dashed line). Cells were either pre-treated with non-targeted shRNA (grey) or Pi4ka targeted shRNA (red). Median fluorescence intensity (MFIR) was calculated as a ratio of MFI relative to shScrmb control. Statistical t-test comparing 3 independent experiments. (* $p \leq 0.05$, ** $p \leq 0.01$ ***, $p \leq 0.001$, ****, $p \leq 0.0001$)

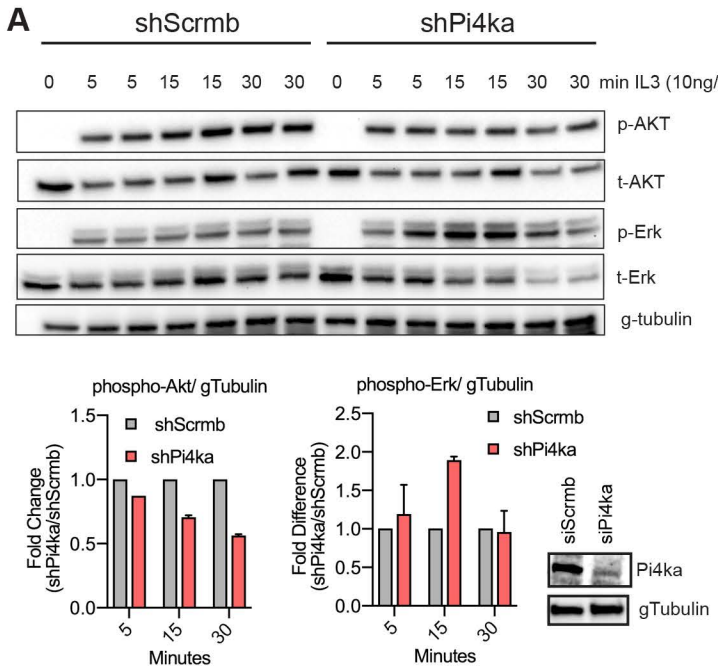

Figure S5. Loss of Pi4ka in vitro blunts Akt signaling and enhances ERK signaling, Related to Figure 6
(A) Western blot assessing AKT and ERK after IL3 stimulation of 32D cells treated with shScrmb or shPi4ka. Cells were treated with 10ng/ml IL3 for 0,5,15, and 30 minutes. Quantification of fold change of shPi4ka treated cells of shScrmb treated cells (bottom). Representative image of Pi4ka knockdown by Western.

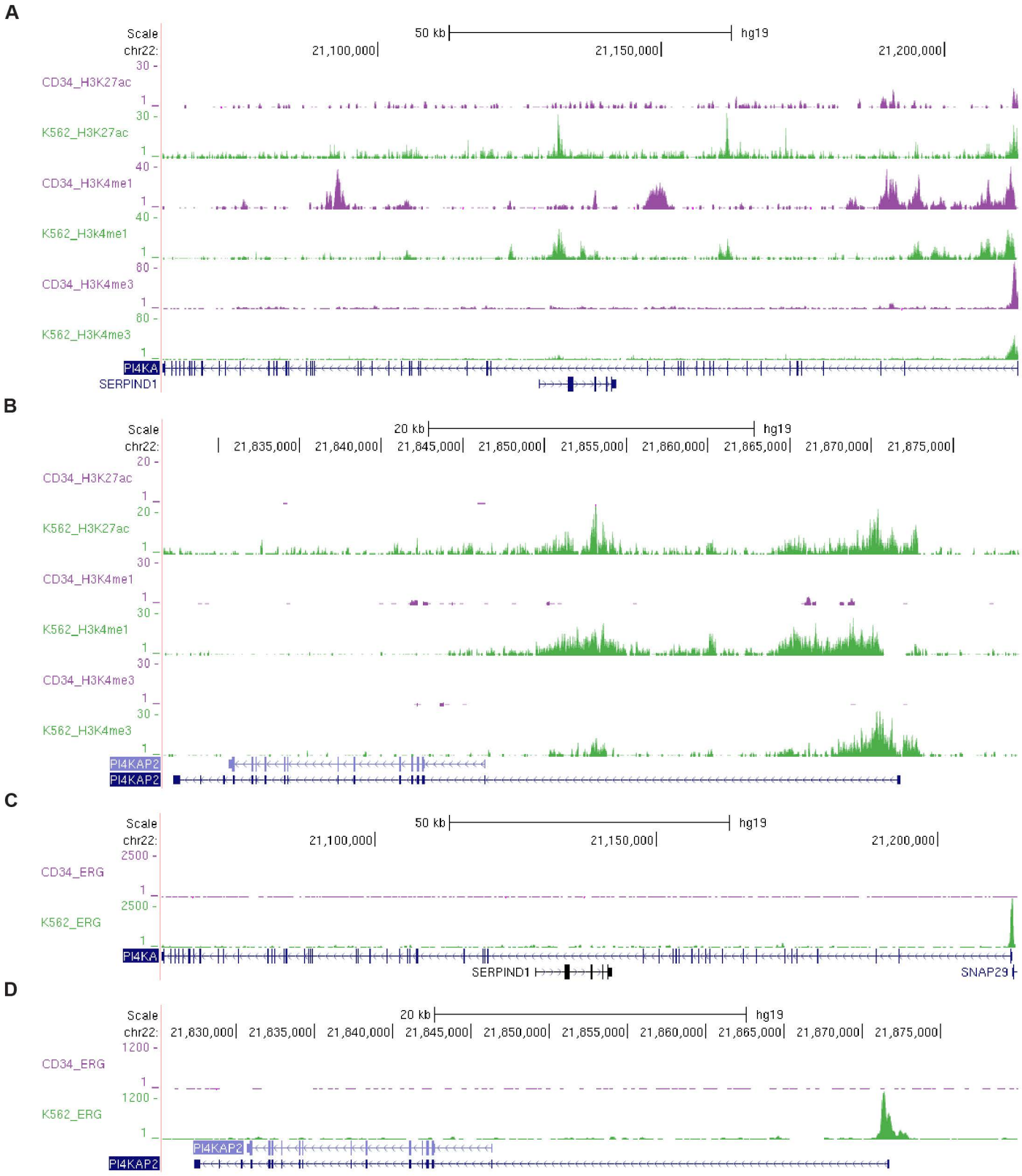

Figure S6. PI4KA and PI4KAP2 promoter transcriptional activation marks and ERG transcription factor binding, Related to Figure 7

(A) UCSC genome browser visualization of transcriptional activation acetylation and methylation marks for the PI4KA gene in human CD34+ HSPC and the human erythroleukemia cell line K562. (B) Transcriptional activaion marks for the PI4KAP2 gene in CD34+ HSPC and eythroleukemia K562 cells. (C) ERG transcription factor binding at the PI4KA promoter in CD34+ HSPC and K562 cells. (D) ERG transcription factor binding at the Pi4kap2 promoter in CD34+ HSPC and K562 cells. (BloodChIP database)

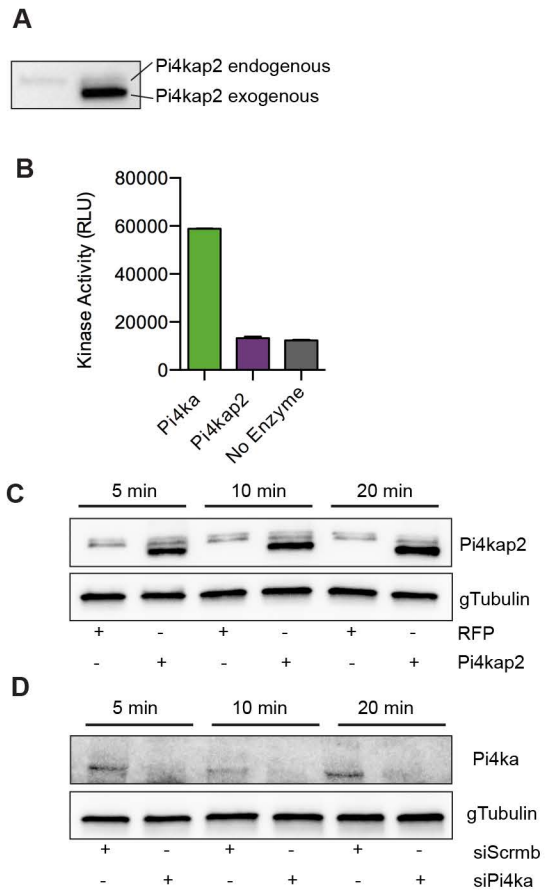

Figure S7. The human Pi4kap2 gene yields protein product, Related to Figure 7
(A) PI4KAP2 construct overexpressed in HEK293 cells. (B) Lipid kinase activity of PI4KA and PI4KAP2. (C) Confirmation of PI4KAP2 and control vector overexpression in HEK293 cells for antibody microarray experiments (D) PI4KA knockdown confirmation in HEK293 cells for antibody micro-array experiments.

Table S1. gCIS captured by VEC-Cre initiated mutagenesis compared to later developmental Cre recombinases, Related to Figure 2

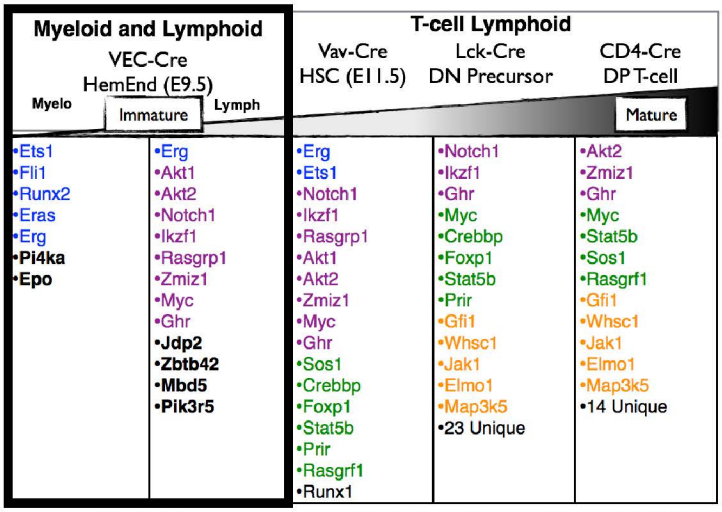

Figure S1: Transposition is unbiased, Related to Figure 2
(A) Plotting the number of hits per chromosome shows that every chromosome is hit by the transposon in both enlarged spleen and thymus tissues. Dotted lines indicate the total number of either spleen and thymus and shows that the majority of these lesions have insertions in all of the chromosomes. (B,C) The total number of insertions per spleen or thymus per chromosome shows there is little influence of chromosome size on number of insertions. Chromosome 4, the transposon donor chromosome, was removed from analysis due to preponderance of local hopping. (D) The average number of insertions per spleen is equal to that of the thymus, yet the average number of gCIS per spleen or thymus is higher in the thymus (E). (F) VEC-Cre initiates mutagenesis during a narrow time window (E9.5-12.5). This is distinct from other Cre initiated and global mutagenesis screens.

Figure S2: Blast-like cells in peripheral blood and bone marrow are associated with gCIS, Related to Figure 2
(A) Mutations in certain gCIS genes were associated with a prevalence of large blast-like immature cells with high nucleus to cytoplasmic ratio in the blood and bone marrow of affected mice. A significant decrease in polymorpho-nuclear cells was observed in the bone marrow of affected animals (scale= 15μm). (arrow= polymorpho-nuclear cell, arrowhead= blast cell) (B) The majority of detected mutation patterns from Figure 2F were associated with very large spleens (3> 800mg, 800>2>500mg, 1<500mg), blast-like cells in the blood, and reduced polymorpho-nuclear cells in the bone marrow of affected animals (each column). M=male, F= female; numbers indicate individual ID number for each mouse.

Figure S3: Pi4ka expression in HSPC budding from HemEnd and in adult lineage negative bone marrow cells, Related to Figure 4.
(A) Pi4ka (red) was observed in the subaortic mesenchyme, but was also found in the membrane of the budding HSPC (CD31 positive, green) from hemogenic E9.5 aorta. (B) Pi4ka (white), CD45 (magenta), and Cdh5-Tomato vasculature (red) immunofluorescence of adult mouse bone marrow. (C) Immunofluorescence of Cdh5-Tomato adult mouse bone marrow with Pi4ka (white) and cKit (blue). (A-C, scale = 10μm) (D) Expression of Pi4ka was higher in HSC (Lin-cKit+Sca1+) and myeloid/erythroid populations of mouse adult marrow when compared to Lin+ differentiated hematopoietic cells. (E) Pi4ka/Pi4kap2 mRNA expression is higher in HSC and myeloid/erythroid lineage human populations in human bone marrow as well as in AML (BloodChIP) Graphs represent mean ± SEM comparisons done by t-test (D) or ANOVA (E). Individual samples are indicated by filled dots.

Figure S4: Loss of Pi4ka decreases erythroid differentiation in vivo and in vitro, Related to Figure 5
(A) Morpholino targeted splicing in the catalytic domain. PCR to assess splicing efficiency. (B) O-dianisidine marking hemoglobin in control and morphant fish. (C) 24 hpf control injected embryos were subjected to flow cytometry and Gata1:DsRED was plotted against Fli1:GFP (left). Histogram of Gata1:DsRED+ cells as a subpopulation of Fli1:GFP cell population. (D,E) Identical gating performed on 48 hour control (top) and morphant embryos (bottom). (F) G1E-ER4 cell differentiation in the presence of 4-hydroxytamoxifen (solid line) or ethanol control (dashed line). Cells were either pre-treated with non-targeted shRNA (grey) or Pi4ka targeted shRNA (red). Median fluorescence intensity (MFIR) was calculated as a ratio of MFI relative to shScrmb control. Statistical t-test comparing 3 independent experiments. (* $p \leq 0.05$, ** $p \leq 0.01$ ***, $p \leq 0.001$, ****, $p \leq 0.0001$)

Figure S5. Loss of Pi4ka in vitro blunts Akt signaling and enhances ERK signaling, Related to Figure 6

(A) Western blot assessing AKT and ERK after IL3 stimulation of 32D cells treated with shScrmb or shPi4ka. Cells were treated with 10ng/ml IL3 for 0,5,15, and 30 minutes. Quantification of fold change of shPi4ka treated cells of shScrmb treated cells (bottom). Representative image of Pi4ka knockdown by Western.

Figure S6. PI4KA and PI4KAP2 promoter transcriptional activation marks and ERG transcription factor binding, Related to Figure 7

(A) UCSC genome browser visualization of transcriptional activation acetylation and methylation marks for the PI4KA gene in human CD34+ HSPC and the human erythroleukemia cell line K562. (B) Transcriptional activaion marks for the PI4KAP2 gene in CD34+ HSPC and eythroleukemia K562 cells. (C) ERG transcription factor binding at the PI4KA promoter in CD34+ HSPC and K562 cells. (D) ERG transcription factor binding at the Pi4kap2 promoter in CD34+ HSPC and K562 cells. (BloodChIP database)

Figure S7. The human Pi4kap2 gene yields protein product, Related to Figure 7

(A) PI4KAP2 construct overexpressed in HEK293 cells. (B) Lipid kinase activity of PI4KA and PI4KAP2. (C) Confirmation of PI4KAP2 and control vector overexpression in HEK293 cells for antibody microarray experiments (D) PI4KA knockdown confirmation in HEK293 cells for antibody micro-array experiments.

Supplementary Experimental Procedures

Lipid Kinase Assay

The Pi4kap2-HA protein was purified from HEK293 cells two days after transient transfection. Cells were lysed with mRIPA buffer and the tagged protein was immuno-precipitated using Pierce anti-HA agarose beads (26181 Thermo Fischer Scientific) in the presence of protease inhibitors overnight. Beads were pelleted, washed with kinase buffer and protein was eluted in kinase buffer supplemented with 1mg/ml HA peptide at RT for 15min. The *in vitro* lipid kinase assay was assembled in a white plate and kinase activity was measured as per the ADP Glo Lipid Kinase Assay Protocol (V6930 Promega). Human Pi4ka (PV5869 Thermo Fisher Scientific) or purified human Pi4kap2-HA was combined with PI:3PS lipid substrate in the presence of ATP for 1 hour. Luminescence was measured using a BMG Labtech Omega plate reader.

Immunofluorescence

For embryos, antibodies against CD31 and Pi4ka were used. Pi4ka staining was followed with biotinylated secondary and amplification was performed by Alexafluor 568 tyramide (Life Technologies). CD31 antibody was followed by Alexafluor-488 conjugated secondary. For adult bone marrow (BM), flushed strands were fixed with PFA, blocked and permeabilized. BM was stained with antibodies against Pi4ka, lineage cocktail, CD45, and fluorescent secondaries (see below). A Zeiss confocal microscope was used to image fluorescence along with Zen acquisition software (Zeiss).

G1E-ER4 differentiation assay

G1E-ER4 cells were pre-treated with non-targeted shRNA or Pi4ka targeted shRNA then FACS sorted based on GFP expression to purify knockdown cell population. Transduced G1E-ER4

cells were then cultured with 0.5U/ml 4-hydroxytamoxifen or ethanol for 48 hours. Differentiation was assessed using anti-Ter119 via flow cytometry.

Antibodies

Primary IHC/IF	**Vendor**	**Catalog #**
Pi4ka	Cell Signaling	4902
CD31	Dianova	DIA-310
Pi4ka	Proteintech	12411-1-AP
V450 lineage cocktail	BD Biosciences	561301
CD45	BD Biosciences	550539
Secondary IF	**Vendor**	**Catalog #**
anti-rat AF-488	LifeTechnologies	A21208
anti-rabbit AF-647	LifeTechnologies	A31573
Primary Western Blot		
phospho- p44/42 MAPK Erk1/2 Thr202/Tyr204	Cell Signaling	9101
total p44/42 MAPK Erk1/2	Cell Signaling	4695
phospho-Akt Ser473	Cell Signaling	9271
total Akt	Cell Signaling	9272
Pi4ka	Proteintech	12411-1-AP
Pi4kap2	Proteintech	16422-1-AP
phospho-S6 Ribosomal Protein Ser240/244	Proteintech	D68F8
beta-Actin	Sigma	
gamma tubulin	Abcam	ab11321

Primers

Morpholino	**Sequence**	**Citation**
pi4kaa splice-inhibitory	5'-AATGTGTGTAACCTTCTGGAAAGCC-3'	(H. Ma et al., 2009)
p53	5' - GCGCCATTGCTTTGCAAGAATTG - 3'	(Langheinrich et al., 2002)
Splicing Efficiency	**Sequence**	**Citation**
zebrafish *pi4kaa* Fwd	5'-GATGGCTCAAAGGGTCTGCTGGCAG-3'	(H. Ma et al., 2009)
zebrafish *pi4kaa* Rev	5'-GTCTCAGTATGGGATTTGGTTCTGG-3'	(H. Ma et al., 2009)
qPCR Primers	**Sequence**	**Citation**
zebrafish *gata1* Fwd	5'-TGAATGTGTGAATTGTGGTG-3'	(Bertrand et al., 2008)
zebrafish *gata1* Rev	5'-ATTGCGTCTCCATAGTGTTG-3'	(Bertrand et al., 2008)
zebrafish PU.1 Fwd	5'-AGAGAGGGTAACCTGGACTG-3'	(Bertrand et al., 2008)
zebrafish PU.1 Rev	5'-AAGTCCACTGGATGAATGTG-3'	(Bertrand et al., 2008)
zebrafish lmo2 Fwd	5'-AAATGAGGAGCCGGTGGAT-3'	(Bertrand et al., 2008)
zebrafish lmo2 Rev	5'-GCTCGATGGCCTTCAGAAA-3'	(Bertrand et al., 2008)
zebrafish scl alpha Fwd	5'-CTGAAATCCGAGCAATTTCC-3'	(Ren et al., 2010)
zebrafish scl alpha Rev	5'-GTTTCCTTGGCAACACCATT-3'	(Ren et al., 2010)
zebrafish mpx Fwd	5'-TGATGTTTGGTTAGGAGGTG-3'	(Bertrand et al., 2008)
zebrafish mpx Rev	5'-GAGCTGTTTTCTGTTTGGTG-3'	(Bertrand et al., 2008)
zebrafish l-plastin Fwd	5'-TGTCTGTGCCCGACACCAT-3'	(Oehlers et al., 2011)
zebrafish l-plastin Rev	5'-GGCGGAGGCAGAGTTCAG-3'	(Oehlers et al., 2011)
zebrafish b-globin e1a/b/c Fwd	5'-CTTGACCATCGTTGTTG-3'	(Ganis et al., 2012)
zebrafish b-globin e1a/b/c Rev	5'-GATGAATTTCTGGAAAGC-3'	(Ganis et al., 2012)
mouse *Pi4ka* Fwd	5'- TTCATGGAGATGTGTGTCCGAGGT-3'	
mouse *Pi4ka* primer Rev	5'- AGGCCTGTGTCCAACATGAGTGTA-3'	
mouse *Rpl7* Fwd	5'- AAGCGGATTGCCTTGACAGA-3'	
mouse *Rpl7* Rev	5'- TTCCTTGAAGCGTTTCCCGA- 3'	
human *PI4KAP1/2* specific Fwd	5'-CAACCATCCGCAATGTGCTTC-3'	
human PI4KAP1/2 specific Rev	5'-GTCAGCTGGGGGAACAAGCT-3'	
human *PI4KA* specific Fwd	5'-GCCTGGAGCATCTCTCCCTA-3'	
human *PI4KA* specific Rev	5'-AGGCACATCACTAACGGCTC-3'	
Molecular Cloning Primers	**Sequence**	
PstI PI4KAP2 Fwd	5'- CTGCAGGTTGGCATGCACCCCCAG-3'	
AgeI PI4KAP2 Rev	5'-ACCGGTTCAGGCGTAGTCAGGAACATCG TAAGGATAGTAGGGGATGTCATTCTGATAG-3'	

MNDU3GFP_Fwd_SphI	5'-GCATGCCAGGGACAGCAGAGATCCAG-3'	
MNDU3GFP_Rev2_MluL	5'-ACGCGTGGTACCGTCGACTGCAG-3'	

Supplemental References

Bertrand, J.Y., Kim, A.D., Teng, S., Traver, D., 2008. CD41+ cmyb+ precursors colonize the zebrafish pronephros by a novel migration route to initiate adult hematopoiesis. Development 135, 1853–1862. doi:10.1242/dev.015297

Ganis, J.J., Hsia, N., Trompouki, E., Jong, J.L.O. de, Dibiase, A., Lambert, J.S., Jia, Z., Sabo, P.J., Weaver, M., Sandstrom, R., Stamatoyannopoulos, J.A., Zhou, Y., Zon, L.I., 2012. Zebrafish globin switching occurs in two developmental stages and is controlled by the LCR. Dev Biol 366, 185–194. doi:10.1016/j.ydbio.2012.03.021

Langheinrich, U., Hennen, E., Stott, G., Vacun, G., 2002. Zebrafish as a model organism for the identification and characterization of drugs and genes affecting p53 signaling. Curr Biol 12, 2023–2028.

Ma, H., Blake, T., Chitnis, A., Liu, P., Balla, T., 2009. Crucial role of phosphatidylinositol 4-kinase IIIalpha in development of zebrafish pectoral fin is linked to phosphoinositide 3-kinase and FGF signaling. J Cell Sci 122, 4303–4310. doi:10.1242/jcs.057646

Oehlers, S.H., Flores, M.V., Hall, C.J., Swift, S., Crosier, K.E., Crosier, P.S., 2011. The inflammatory bowel disease (IBD) susceptibility genes NOD1 and NOD2 have conserved anti-bacterial roles in zebrafish. Disease Models & Mechanisms 4, 832–841. doi:10.1242/dmm.006122

Ren, X., Gomez, G.A., Zhang, B., Lin, S., 2010. Scl isoforms act downstream of etsrp to specify angioblasts and definitive hematopoietic stem cells. Blood 115, 5338–5346. doi:10.1182/blood-2009-09-244640